Climate Changes, Impacts and Implications for New Zealand to 2100

Synthesis Report: RA2 Coastal Case Study

The Firth of Thames and Lower Waihou River

G McBride[1], G Reeve[1], M Pritchard[1], C Lundquist[1], A Daigneault[2], R Bell[1], P Blackett[1], A Swales[1], S Wadhwa[1], A Tait[3], C Zammit[4]

[1] National Institute of Water & Atmospheric Research Ltd, Hamilton, New Zealand
[2] Landcare Research Ltd, Auckland, New Zealand
[3]National Institute of Water & Atmospheric Research Ltd, Wellington, New Zealand
[4]National Institute of Water & Atmospheric Research Ltd, Christchurch, New Zealand

**Corresponding author, email: Graham.McBride@niwa.co.nz*

Present-day LiDAR bathymetry of the Firth of Thames intertidal zone, overlaid by mangrove distribution

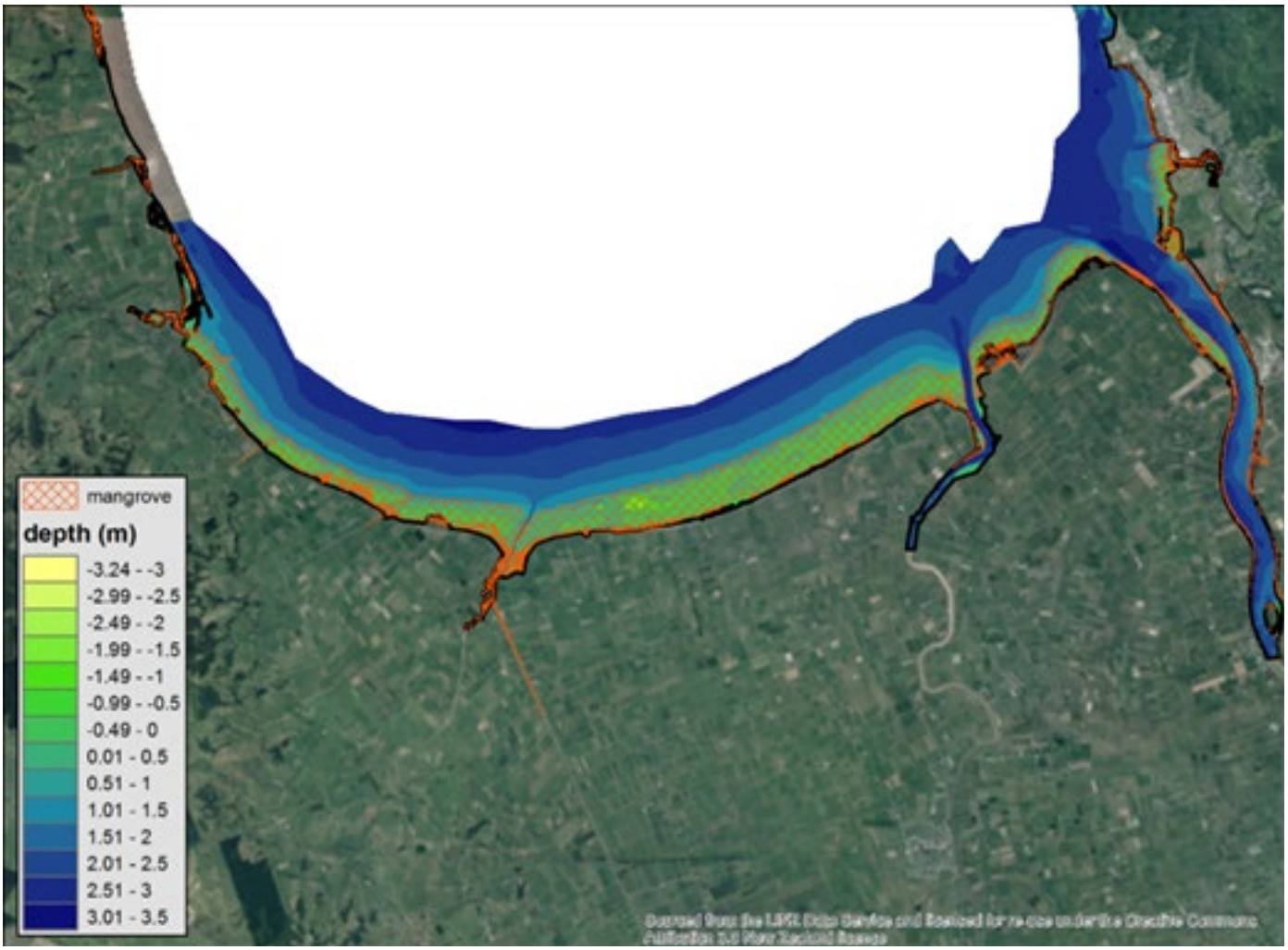

When quoting, citing or distributing this Report or its individual sections, please provide the full reference: McBride G, Reeve G, Pritchard M, Lundquist C, Daigneault A, Bell R, Blackett P, Swales A, Wadhwa S, Tait A, Zammit C (2016) *The Firth of Thames and Lower Waihou River*. Synthesis Report RA2, Coastal Case Study. Climate Changes, Impacts and Implications (CCII) for New Zealand to 2100. MBIE contract C01X1225. 50pp.

Cover photo: Ray J Salisbury, www.mychillybin.co.nz

CONTENTS

HIGHLIGHTS

Firth of Thames water levels and depths

- Sea level rise (SLR) will result in increased flooding of shore communities
- Water depths in the Firth over time are projected to be relatively independent of RCP values (with rate of sea level rise roughly in tandem with sedimentation), but will nevertheless be maximal for RCP 8.5 (high greenhouse gas emissions)
- Areas of wetting and drying in the Firth may increase over time, particularly if more intense land uses evolve, making navigation more difficult
- Conversely, there would be less wetting and drying were widespread reforestation to be adopted in the contributing catchments

Firth of Thames mangrove distributions projections

- Under present landuses, up to 100% increase in mangrove habitat is projected in suitable areas, with a decrease of habitat in subtidal areas
- For a 20% reduction in sediment supply (e.g., because of reforestation) some reduction in suitable habitat can be expected, especially for areas presently marginal for mangrove production
- For a 20% increase in sediment supply (e.g., because of intensified landuses) a general increase in suitable habitat is projected

Waihou and Piako River flows

- Projected changes in river flows are strongly linked to projected changes in precipitation
- The median change in the annual mean flow is relatively small, with generally negative changes in winter and summer (decreased mean flow) and positive changes in spring and autumn (increased mean flow)
- Uncertainty in flow projections is high, corresponding to similar uncertainty in future precipitation projections for this region

Waihou River salinity intrusion and flooding

- SLR is the main contributor to changes in saline intrusion and flooding
- Salinity intrusion up the Waihou River is projected to extend up to a further 5 km inland (for a 1 metre SLR over the next century), and is relatively unaffected by changes in low river flows
- Flooding in the upper part of the river (>50 km from the Firth) is largely unaffected by SLR
- The largest impact of SLR and flood interaction will occur in the lower Waihou River (between Pekapeka and Puke Bridge), with up to a 0.5 m increase in combined flood level at Pekapeka for a 1 m SLR

Economic and land use scenario analysis

- Agricultural commodity prices vary significantly over time due to changes in global socio-economic conditions, population growth, and climate change policy.
- Primary production is estimated to increase regardless of which Representative Concentration Pathway (RCP) is modelled. Forestry yields increase the most due to the influence of an increase in atmospheric CO_2.
- A scenario of increased sediment loads is driven by deforestation and a shift to pastoral land uses
- A scenario of a decline in sediment loads can be attributed to high carbon prices shifting marginal sheep and beef land to pine plantations, scrub, and fallow land.

The results giving rise to these highlights are given in the main body of this report; various technical explanations are given in the Appendix.

INTRODUCTION AND BACKGROUND

The CCII project

The "Climate Changes, Impacts and Implications" (CCII) project is a four-year project (October 2012 – September 2016) designed to address the following question:

What are the predicted climatic conditions and assessed/ potential impacts and implications of climate variability and trends on New Zealand and its regional biophysical environment, the economy and society, at projected critical temporal steps up to 2100?

The CCII project brings together a strong research team with knowledge and modelling capabilities in climate, ecosystems, land and water use, economics, and sociocultural research to address the environment sector investment plan priority of "stronger prediction and modelling systems".

The project is based around five inter-related Research Aims (RAs) that will ultimately provide new climate change projections and advancements in understanding their impacts and implications for New Zealand's environment, economy and society. The five RAs are:

Research Aim 1: *Improved Climate Projections*

Research Aim 2: *Understanding Pressure Points, Critical Steps and Potential Responses*

Research Aim 3: *Identifying Feedbacks, Understanding Cumulative Impacts and Recognising Limits*

Research Aim 4: *Enhancing Capacity and Increasing Coordination to Support Decision-making*

Research Aim 5: *Exploring Options for New Zealand in Different Changing Global Climates*

The overall purpose of RA2 is to: Perform five case studies on the potential impacts of climate change and other key drivers on alpine, hill & high country, lowland, coasts & estuaries, and marine environments. This synthesis report presents the results of the coastal case study.

Coastal climate change and sea-level rise

In the modern era, global sea level began to rise around the latter half of the 1800's, and steadily increased at a rate within the range 1.4–1.9 mm per year during the 20th century.

Across New Zealand, the average relative (local) sea-level rise from 1900–2015 is 1.78 ± 0.21 mm per year and, since 1961, is 2.14 ± 0.47 mm per year (MfE, 2016), results that are very similar to those given in Church and White (2011) for global averages. This means that projections for global sea-level rise can generally be adopted, provided allowances are made for regional and local differences.

In the satellite era (since 1993), global mean sea level has risen by 3.3 mm per year, attributable partly to natural climate variability and partly an acceleration in sea-level rise due to warming of the atmosphere and oceans.

Key drivers of the rise in sea level are:

- Thermal expansion from warming ocean waters
- Additional water mass added to the ocean from glaciers, ice sheets and net freshwater runoff
- Vertical land movement can substantially alter the local sea-level rise, with any land subsidence compounding the ocean rise

Locally, it is the local or relative sea-level rise that need to be adapted to – not the global average rate. However projections of future sea-level rise are usually based on global projections. So for New Zealand, offsets need to be applied to projections for differences in the regional-ocean response for the Southwest Pacific (e.g., a modest additional 0.05 m by the 2090s – Ackerley et al., 2013) and local vertical land movement (which can be measured by continuous GPS recorders).

IPCC projections (5th Assessment Report, WGI, Chapter 13, Church et al., 2013) of global sea-level rise by 2100 cover a range of around 0.4–1 m, depending on the Representative Concentration Pathway (RCP). The

range in sea-level rise projections is much narrower in the near-term to 2060 (0.3–0.4 m). However, beyond 2100, the spectre of runaway instabilities of polar ice sheets in West Antarctica and Greenland, if global temperatures exceed a threshold of ~2°C above pre-industrial levels (Golledge et al., 2015), considerably increases the range of possible future sea-level trajectories to consider in planning and design.

Small increases of the order of 1–5% in wave height and storm surges from climate change effects are also likely by 2090 (NIWA WASP project, unpublished).

Projected climate changes for the Waikato region

A complete assessment of updated climate change projections for New Zealand, based on data described in the CCII RA1 Synthesis Report, has recently been performed by NIWA for the Ministry for the Environment (MfE, 2016)[1]. This report includes projections for the middle and end of the century, incorporating results from multiple climate models and four "Representative Concentration Pathways" or RCPs. The RCPs represent estimated changes in radiative forcing resulting from greenhouse gas concentration trajectories under different socio-economic assumptions. The RCPs describe four potential climate futures (see Appendix, Figure 22); RCP2.6 represents a low-emission mitigation pathway, requiring removal to achieve a decline in atmospheric CO_2 by 2050, whereas RCP8.5 is the high emission scenario. The two middle pathways (RCP4.5 and 6.0) require stabilisation of emissions at different time points during the 21st Century.

For the Waikato region, the following "snapshot" of future climate changes by the end of the century (compared with the present-day) is based only on RCP8.5 and the average of several climate models. For more detailed information, the reader is directed to the MfE report.[1]

- Increase in the mean air temperate (°C): Summer 3.3; Autumn 3.2; Winter 3.1; Spring 2.7
- Change in the mean precipitation at Ruakura (%)[2]: Summer +3; Autumn -3; Winter +5; Spring -6
- Increase in the number of "hot days" ($T_{max} \geq 25°C$): Present-day 23.6 days per year; End of century 84.0 days per year
- Decrease in the number of "cold nights" ($T_{min} \leq 0°C$): Present-day 15.2 nights per year; End of century 1.9 nights per year
- Increase in the number of "dry days" (Precipitation < 1 mm/day) by 5-10 days per year
- Increase in the 99th percentile rainfall amount (approximately equal to the heaviest 24-hour rainfall each year) by 5–10%
- Decrease in the 99th percentile wind speed (approximately equal to the third highest average daily wind speed each year) by 0–5%
- Increase in drought intensity/duration, as indicated by an increase in Potential Evapotranspiration Deficit (amount of water needed for irrigation) by 50–100 mm per year (approximately 25-35% increase from present-day)

[1]http://www.mfe.govt.nz/publications/climate-change/climate-change-projections-new-zealand
[2]There is a large range of projected precipitation changes for this location, depending upon the climate model. Furthermore, precipitation changes vary spatially across the region (see http://ofcnz.niwa.co.nz)

CASE STUDY SELECTION AND STAKEHOLDER ENGAGEMENT

Range of expected impacts and implications on estuaries and coasts

By the middle of this century water and air temperatures are expected to be, on average, around a degree Celsius higher than was the case in the 1990s, and sea level rise is expected to be 25–35 cm. Toward the end of the century the temperature increment may be as high as 4–5°C and sea level may have risen by 50 to 80 cm or more. Average annual rainfall is generally expected to increase in the west and south of New Zealand, and decrease in the east and north, and heavy rainfall events may become more severe.

Associated impacts include: ground-water salinization of coastal aquifers; changes in tide range; enhanced upstream saline intrusion affecting potability of water supplies and suitability for irrigation; changes in estuarine ecosystems (e.g., through drowning of intertidal reefs); changing temperature and aquatic plant habitat effects on kai moana; changes in estuarine sedimentation and consequent effects on ecosystem health; changing underwater light regimes; impacts on ICOLLs (Intermittently Closed and Open Lakes and Lagoon) and river mouths; land drainage and stormwater management in low-lying land; shoreline erosion; microbial water quality changes affecting public health); drainage and stormwater systems; bank erosion; river flood control measures (e.g., willow management, outflanked by sea level rise); changing effect on river cuts or partial diversions, bridges and road/rail infrastructure.

Two broad areas of impacts in the estuarine and coastal areas may be foreseen: *physical hazards* (from sea level rise and flooding) and changes in *coastal habitat distribution* (e.g., mangroves/seagrasses/reefs, from sea level rise, sedimentation and temperature effects).

Implications range from a requirement to reinforce or move infrastructure (roads, bridges, water supplies, fencing) to concerns about continued availability of kai moana—shoreline food gathering by Iwi and others.

Case study selection—stakeholder engagement

In order to identify potential coastal case study areas the research team compiled a nation-wide short list of options which were assessed against several key criteria; access to existing scientific data and models, potential significance of climate change impacts, and current relationships with local stakeholders. As the two most preferred potential locations were within the Waikato Region, a meeting with the Regional Council was convened in December 2013 to jointly select the case study area. Through this discussion, the lower Hauraki Plains and Firth of Thames were identified and an initial research plan was constructed.

A further workshop occurred in Hamilton on 8 May 2014 which brought together organisations and agencies whose interests and activities could be affected by climate change in the case study area. Participants included representatives from the Department of Conservation (1), New Zealand Landcare Trust (1), DairyNZ/Fonterra (2), Thames Coromandel District Council (1), Auckland Council (2), Rural Women's Network (1), Federated Farmers (1), and Waikato Regional Council (3). The purpose was to introduce the proposed research, refine the proposal based on what was important to the stakeholders, identify complementary sources of data or models and spatially locate the potential wider impacts and implications of climate change using large aerial photos (Figure 1).

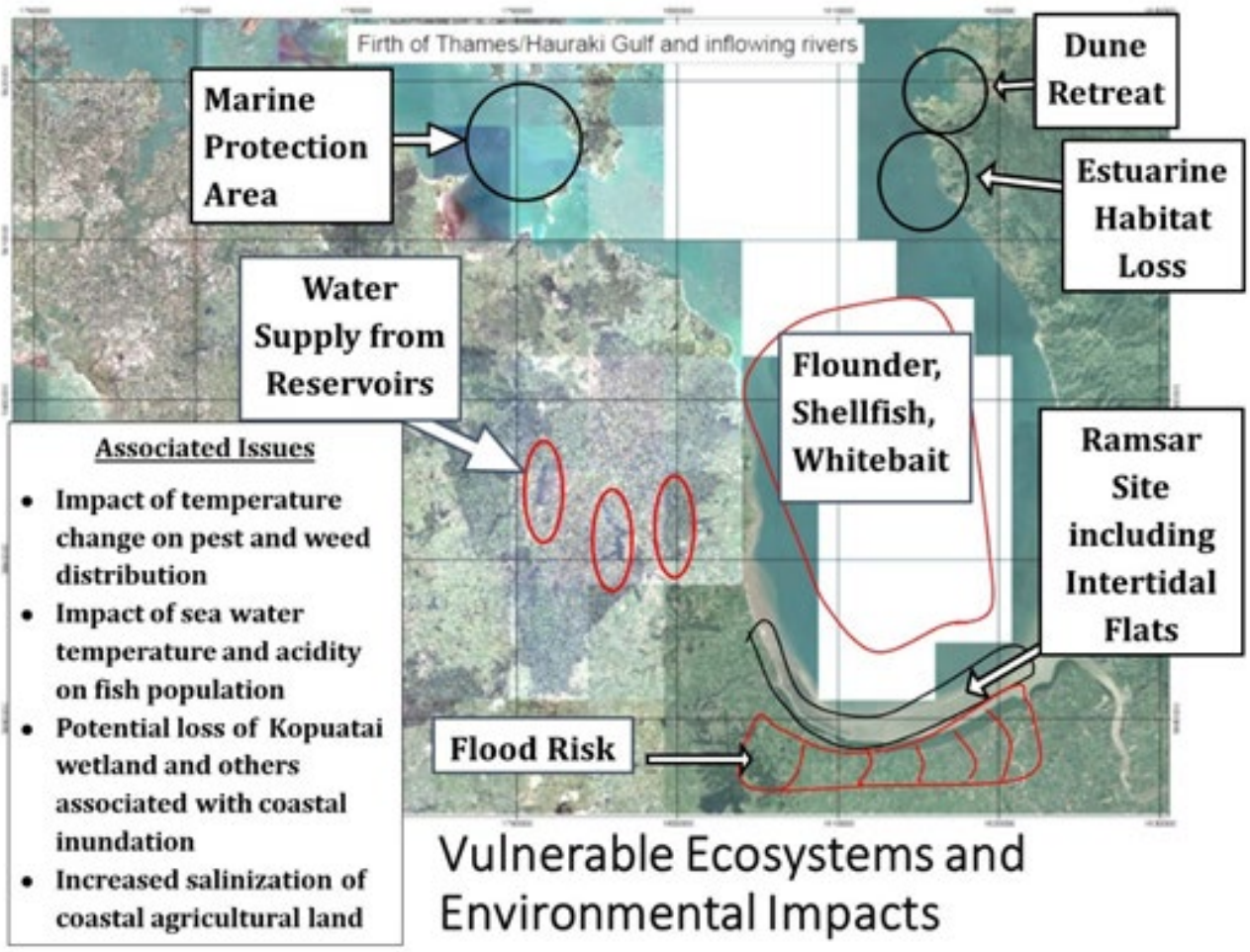

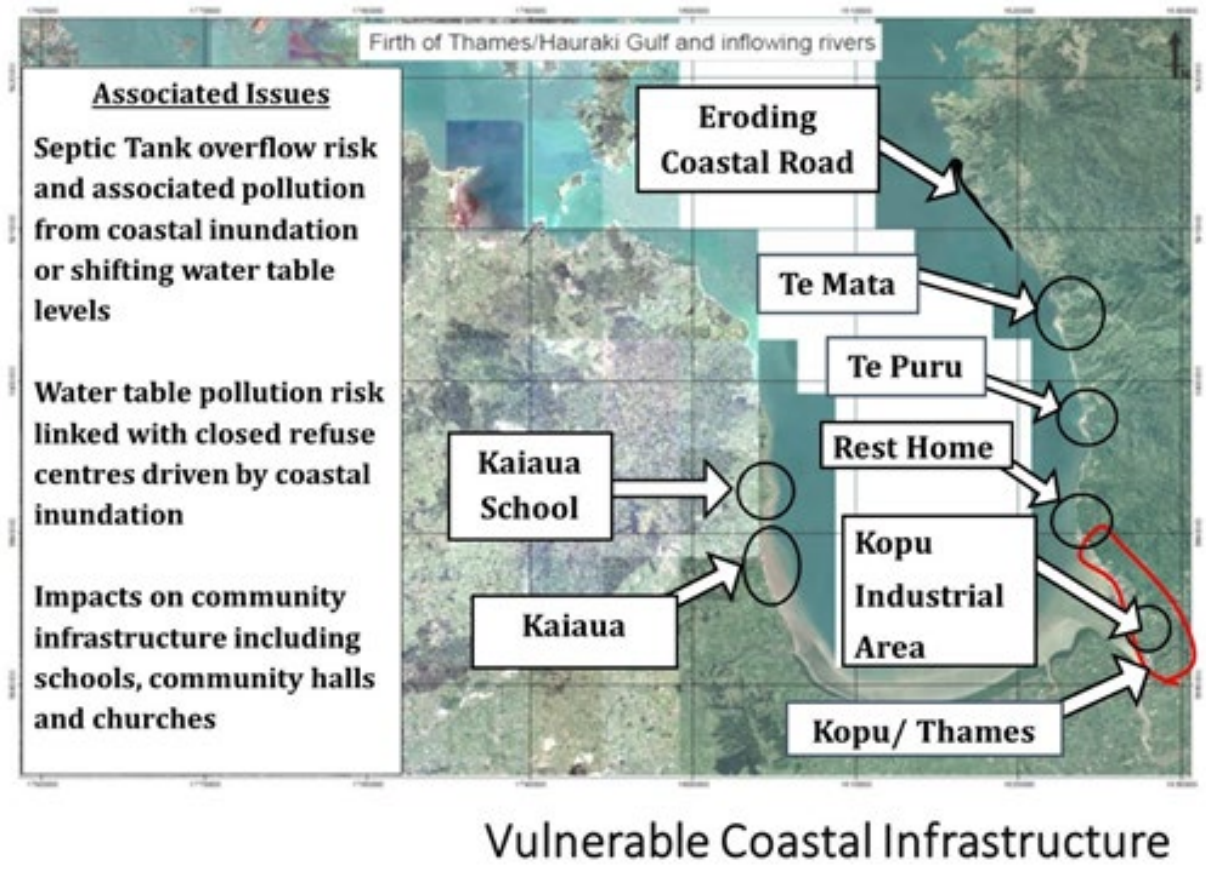

Figure 1 Range of impacts and implications for the study area.

The stakeholders identified a wide range of potential impacts and implications of climate change including: aquaculture and seawater pH changes (e.g., impacting shellfish spat); regional economics; freshwater fish; Hauraki plains infrastructure (roads, drainage, engineering lifelines, private property, community assets and commercial property); coastal wetlands/marshes; sediment-associated risks to the southern and south-western coast and intertidal zone of the Firth of Thames, an area recognised as an internationally important wetland under the Ramsar Convention; inundation/flooding hazards; climate change effects on landslips, rainfall intensity, droughts, groundwater (quality and effect on drainage from rising water tables and liquefaction risk); community resilience; Piako River—maybe more of an issue than Waihou (water allocation/salinisation effects on Kerepehi water supply; resource management decisions including ecosystem services; irrigation (increased demand and allocation if more droughts); and inland seawater intrusion.

Final selection

After these consultations, and taking stock of the resources available to the project team, we modelled a selection of the above potential impacts for both aspects (*Hazards and Habitats*) in the Firth of Thames and associated contributing catchments, particularly the Waihou River catchment.

Background to that choice – Hazards

Most past New Zealand research has focussed on open coast systems where land and freshwater effects were ignored[3]. The Firth of Thames and Waihou River is one of the study sites in the Natural Hazards Platform (NHP) storm-tide project, so we have chosen to model of tidally-affected section of the lower Waihou River and Firth, linking them via hydrodynamic models. The Firth/rivers system is in national and regional spotlight, primarily regarding catchment run-off but also the growing exposure to coastal/river flooding. It will also bear the brunt of climate change impacts because of the very low-lying terrain of the Hauraki Plains (drainage issues, inundation hazards), and salinisation (bank vegetation, Paeroa water intake already subject to salinization on high spring tides). The effects of changes in rainfall intensity may also be critical.

Background to that choice – Habitats

New Zealand mangrove forests benefit coastal and estuarine ecosystems in a myriad of ways, functioning as long-term sinks for stormwater contaminants (e.g., fine sediments, stormwater contaminants, nutrients) and carbon, and support biodiversity and detrital food-webs through primary production. NZ mangrove forests also have the capacity to mitigate coastal erosion and inundation hazards associated with local wind and swell waves and storm tides. This ecological service has been documented for the southern Firth of Thames (Figure 2).

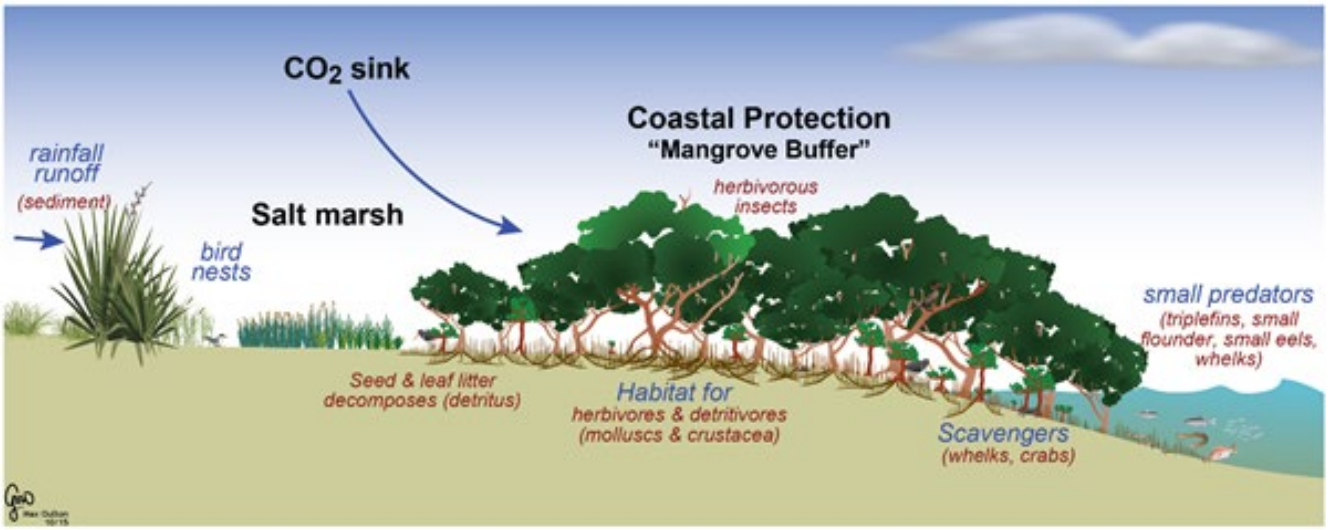

Figure 2 Ecological services provided by mangrove forests.

[1]The CACC (Coastal Adaptation to Climate Change) community consultation mapping is an exception: simple mapping of possible impacts on estuary mangroves and saltmarsh in Whitianga estuary (see http://www.niwa.co.nz/coasts/update/coasts-update-03-april-2011/preparing-coastal-communities-for-climate-change). This included doing a comparison of CC impacts on Whitianga (coastal resort) vs Manaia (coastal Māori community).

Coastal case study description

The Firth of Thames is an 800 km^2 estuarine embayment occupying the Hauraki Depression bounded to the east and west by the Coromandel and Hunua Ranges (Swales et al. 2015, Green & Zeldis 2015). It has a contributing catchment of 3600 km^2 in a temperate climate with an average minimum winter air temperature of about 10°C and average maximum of about 20°C in summer. Mean monthly rainfall varies from 73 mm (summer) to 145 mm (winter), with a mean annual rainfall of about 1200 mm.

Prior to human habitation the Hauraki Plains was mainly native forest-clad but is now dominated by agricultural land use. The Firth receives runoff primarily from the Waihou and Piako Rivers. Tidal and wind-driven currents, mixing, and stratification are important hydrodynamic processes that influence all biogeochemical processes in the Firth of Thames and the wider Hauraki Gulf.

Fine sediments have already impaired and continue to affect ecosystem health in the Firth, originating from historical land clearance and mining operations in tributaries in the late 1800s to early 1900s. Present-day inputs of sediment from these rivers account for only 40% of the estimated 430,000 t y^{-1} of sediment currently depositing in the southern Firth of Thames (Green & Zeldis 2015). The apparent discrepancy is likely to be due to the reworking by waves and currents of legacy sediments. Sediments are now accumulating at rates 2–10 times greater than 90 years earlier.

Mangrove forest (*Avicennia marina* var. *australasica*) has colonized 11 km^2 of intertidal flat in the southern Firth since the early 1960s, occurring close to the southernmost global mangroves limit. Mangrove-forest expansion is a recent phenomenon with mangrove trees restricted to river deltas until as recently as the early 1950s. The mangrove forest that has developed along the southern Firth shore occupies an 800 m wide zone on an upper-intertidal platform.

The Hauraki Plains south of the Firth are underlain by marine sediments that were covered by freshwater marshes and Kahikatea (*Dacrycarpus dacrydioides*) swamp forests when Maori first arrived.

METHODOLOGY

A key feature of climate change studies is that there are multiple socio-economic pathways to achieving similar levels of greenhouse gas emissions and hence changes in key environmental physical variables: rainfall, runoff, wind and temperature. Therefore, one must also consider changes in public policies at multiple scales. For example, sediment input to the Firth of Thames may be analysed for a particular rate of sea-level rise but under at least two scenarios: (a) intensive and poorly-controlled sediment runoff versus (b) reforestation. Both options need consideration. The impacts of changed sediment delivery, for a given RCP, may be substantial. We explore that feature in this case study.

Models used

For the biophysical modelling these comprise:

- Computational 3D hydrodynamic TELEMAC3D code (freeware) for river flooding and salinity intrusion[4]
- Computational 3D Deltares proprietary code for coastal sedimentation and associated hydrodynamics[5]
- A new Water Column Model for sediment deposition over multiple tidal cycles, based on recent work by Marani et al. (2010) and discussed with Professor Giovanni Coco (Auckland University); see the Appendix
- TOPNET hydrological model for catchment flows[6]
- Coastal habitat layers sourced from Waikato Regional Council layers prepared for Sea Change - Tai Timu Tai Pari (Hauraki Gulf Marine Spatial Plan, updated in 2013) based on aerial photograph analysis (Waikato Regional Aerial Photography Service (WRAPS))
- LiDAR bathymetry based on Moturiki datum, data sourced from Waikato Regional Council (Waikato Regional Council & NZ Aerial Mapping Ltd. 2012 – 2013 licensed under Creative Commons 3.0 NZ)

The models used for the economic and land use scenarios are listed in Table 1.

Computational hydrodynamic models

The essence of these models lies in solving fundamental fluid dynamics equations on user-defined 'grids' taking particular account of wind shear and direction and projected sea level rise and 'boundary conditions'. The grid used for the TELEMAC3D model is shown in Figure 23 (Appendix); as can be seen it divides the bed into a large number of much smaller elements.

Sediment models

Most terrestrial fine sediment eroded from New Zealand catchments is transported from the land via a river to an estuary during storm events. The duration, runoff and storm frequency largely determines the sediment load input to the estuary. Whereas once in the estuary basin, the tide, wind and wave interaction with existing morphology will largely determine where the sediment will move, deposit or later erode. Due to the long-term uncertainties in the empirical parameters used in 2-D or 3-D models plus the limitations of computer memory, using these complicated models to predict estuarine morphological development over climate change time scales is not a

Table 1. Economic and land use scenarios models.

Domain	Model	Indicator
Population	Population model output (Cameron, 2013)	Demographic
Economic development	Climat-DGE (Fernandez & Daigneault, 2015)	Commodity prices downscaled to New Zealand
Primary production	cenW (forestry) (Kirschbaum et al., 2012) BiomeBGC (pasture) (Keller et al., 2014)	Yield change Yield change
Land-use change	NZFARM (Daigneault et al., 2014)	Change in land use area and associated environmental outputs
Erosion	NZeem (Dymond et al, 2013)	Sediment loss due to land cover changes

[4]http://www.opentelemac.org/index.php/presentation?id=18
[5]https://oss.deltares.nl/web/delft3d/about
[6]https://teamwork.niwa.co.nz/display/IFM/Topnet

very practical option. This became particularly evident for the CCII project where the impact of several RCP's predicted by several different climate models on estuarine morphology were being compared.

To get around this problem we take a 2-tier modelling approach. Firstly we use a 3-D (Deltares) hydrodynamic and sediment transport model of the Firth of Thames estuary to predict were sediments sourced from event scale (~3-days) buoyant river plumes disperse and deposit in the estuary basin. Then the resultant predicted sediment dispersal footprint, which, is based on tides, winds and plume dynamics, is used to locate the intertidal and subtidal sites that will receive a sediment supply. We then investigate the long term morphological evolution at these sites using different climate models and RCP's for a period of 100+ years.

The Water Column Model predicts the temporal evolution (through sedimentation) of a tidal platform (sea bed) elevation (relative to datum) over long time scales through a zero point (Water Column Model) approach. The model can be 'moved around' an estuary and can be set on either an inter-tidal flat or sub-tidal channel. The model can be run at points over a cross shore transect of and estuary channel i.e. from sub-tidal to upper mudflat.

The model includes drying and wetting meaning that sediment can only be supplied, deposited and or eroded when the platform is covered by the tide and sediment delivery is assumed constant. The sediment settling (deposition) is computed from a term that is based on settling velocity of the sediment particles, sediment concentration and trapping by vegetation over a flooding (delivery) and ebbing (export) tide.

Sediment erosion on the platform by wind waves is calculated from wind speed magnitudes for each RCP and distance of fetch (distance across the Firth) is used to compute wave length and period that is then used to estimate a wave orbital driven bed shear stress. If the bed shear stress exceeds a critical threshold (based on sediment rheology), the bed erodes. The rate of regional mean sea-level rise included in simulations is based on the predicted rate for each respective RCP. The sediment flux (+ or –) is integrated over a tidal period and the cumulative platform level change (z) after each tide is used as the start height of the platform for the next tidal cycle. The model includes the effects of sea-level rise and trapping by vegetation.

TopNet

The TopNet hydrological model is routinely used for hydrological modelling applications in New Zealand. It is a spatially distributed, time-stepping model of water balance driven by time series of precipitation and temperature data, and of additional weather elements where available. It produces time series of modelled river flow (under natural conditions) throughout the modelled river network. TopNet model equations and information requirements are provided by Clark et al. (2008) and McMillan et al. (2013). Calibrated hydrological models (See Appendix section 10.5) were built for the eight surface water catchments based on Strahler 1 catchments (typical size 0.7 km^2) presented in Figure 3.

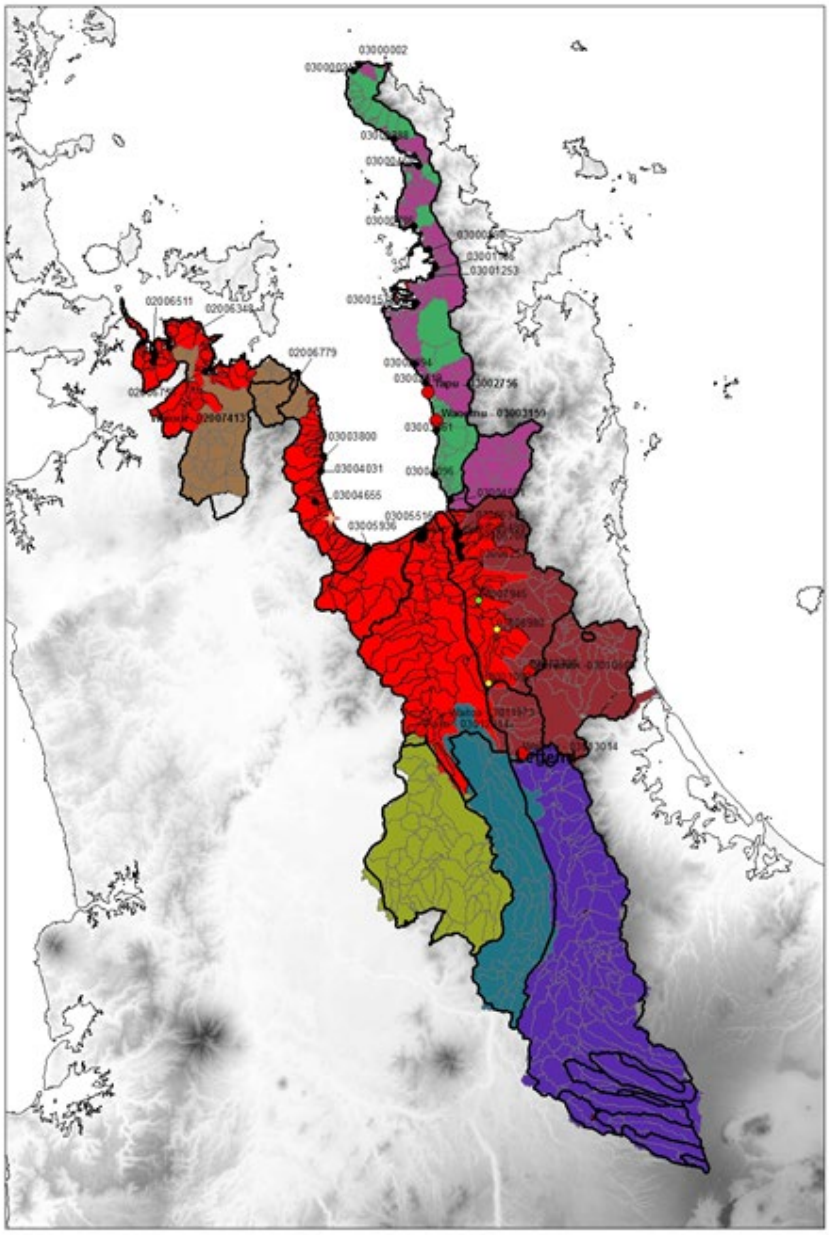

Figure 3 TopNet surface water model extent. The different colours represent the different TopNet basins. Reporting locations are identified by their river Strahler number.

Mangrove cover modelling

Analysis of historical information show that New Zealand mangrove-forests have expanded their range at an average rate (4% yr^{-1}, range 0–20% yr^{-1}) twice that observed for the same species (*Avicennia marina*) in south-east Australia over the last 150 years under a regime of increased catchment soil erosion and accelerated estuary infilling (Morrisey et al., 2010).

Mangrove forests occupy the intertidal zone above mean sea level (MSL) elevation. This lower-elevation threshold primarily relates to the physiological tolerance of mangrove (seedlings in particular) to emersion. Regular daily exposure to the air enables seedlings growing in muddy substrates in particular to maintain an adequate oxygen supply to their tissues. In this way, tidal-flat surface elevation exerts a first-order control on mangrove-forest distribution.

Because mangrove forests occupy a narrow elevation range and must maintain their position within the intertidal zone they are sensitive to changing sea level. Thus, the long-term fate of mangrove forests depends on tidal-flat surface elevation increasing at a rate equal to or exceeding the rate of sea-level rise (SLR). Over geological time scales, mangrove-forest response to eustatic sea-level fluctuations depends on local relative SLR (i.e., vertical land movement), climate-change effects on mangrove productivity, and sediment supply from rivers. For example, early Holocene mangrove forests were inundated as they were unable to keep pace with rapid SLR of 5–15 mm yr^{-1}. (The rate of SLR predicted for New Zealand by 2100 is within this range). Mangrove distribution is also sensitive to wave exposure and other oceanographic processes (e.g., storm surge, wave climate), which dislodges seedlings

(Balke et al. 2015). Periodic expansion events of mangroves the Firth of Thames have been associated with climatic regimes with longer periods of low wave energy during the seedling establishment period (Lovelock et al. 2010).

Modern mangrove forests have, in general, adapted to mean eustatic SLR of 1.7 mm yr^{-1} (IPCC 2007) over the last century through vertical accretion of mineral and/or organic sediments. There is uncertainty about the capacity of mangrove-forests to respond to predicted rates of SLR of up to 10 mm yr^{-1} during the next century.

Distributions of mangrove forests and other coastal vegetation layers were available from Waikato Regional Council based on aerial photograph analysis, updated in 2013 for the Sea Change – Tai Timu Tai Pari (Hauraki Gulf Marine Spatial Plan). As mangrove expansion in the Firth of Thames typically occurs on approximately decadal scales associated with El Niño events (Lovelock et al. 2010), this distribution layer was assumed accurate to 2013.

Mangrove distribution was overlapped with LiDAR depths based on Moturiki Vertical Datum 1953 (MVD-53), with area calculated across each 25 cm incremental depth bands from approximately 3 m above to 3 m below datum (Figure 4).

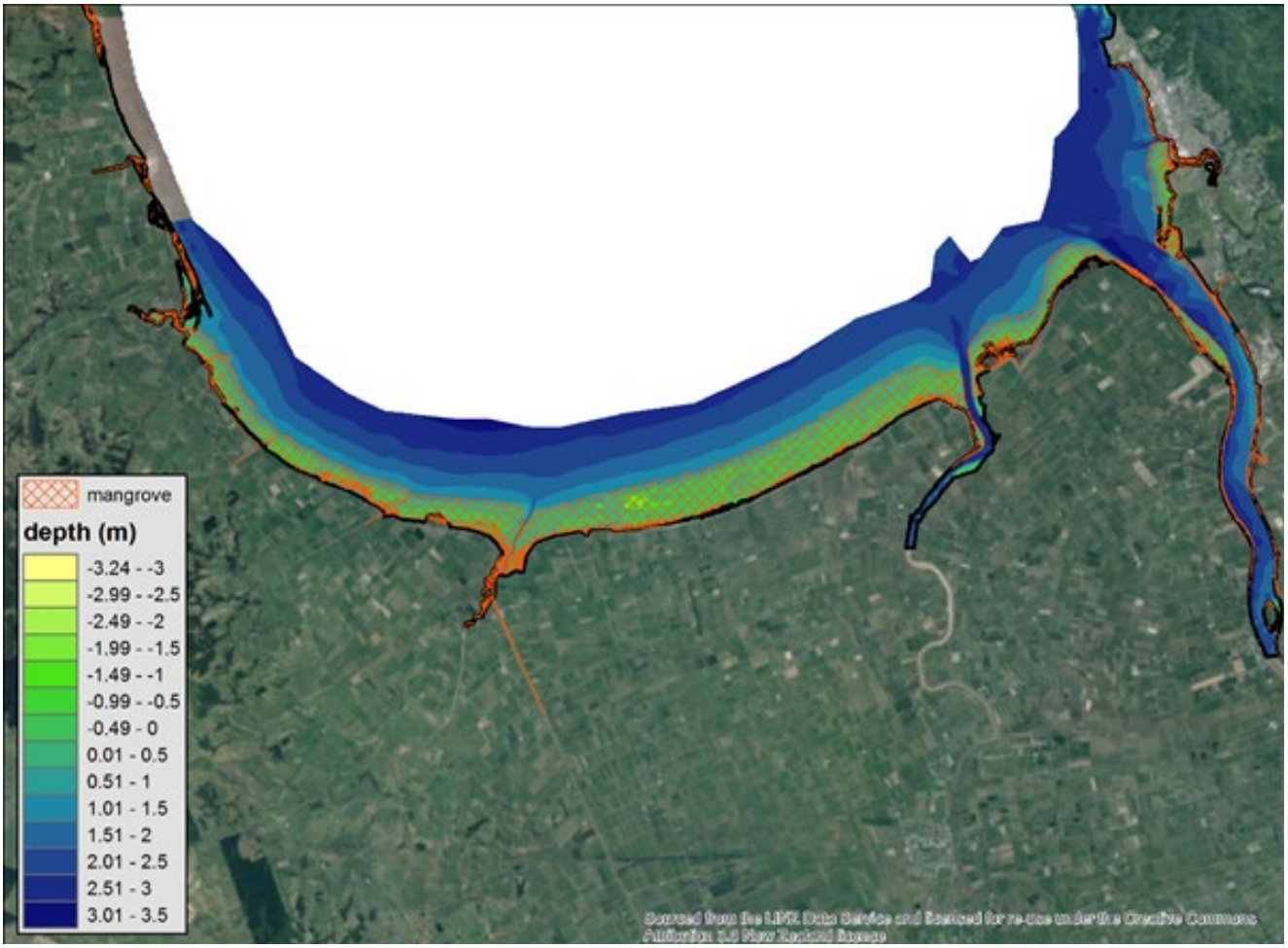

Figure 4 Present-day LiDAR bathymetry of the Firth of Thames intertidal zone, overlaid by mangrove distribution. Depths are relative to Moturiki datum, with positive values being above mean sea level, and negative values being below mean sea level.

Spurious LiDAR depth outliers were corrected in the intertidal zone, typically due to LiDAR analysis errors due to the presence of large mangrove trees in the upper intertidal zone. To allow estimation of change in bed level height based on the Deltares model, depths were converted to depth bands representing four coastal habitat suitability classes: 1) Saltmarsh: saltmarsh dominated depths above upper intertidal limit of mangrove current distribution, corresponding to depths > 2 m above Moturiki datum; 2) Mangrove Upper: highly suitable depths for mangroves, corresponding to depths from 2 m above to 1 m below Moturiki datum; 3) Mangrove Lower: low suitability for mangroves where depth is within depth range suitable to mangroves (i.e., greater than mean water depth, submerged less than half of the tidal cycle) but wave exposure limits colonisation success to approximately 10% of this suitable habitat, corresponding to depths between 1 m below to 2 m below Moturiki datum; and 4) Subtidal: depths currently unsuitable for mangroves, i.e., below mean sea level, corresponding to depths > 2 m below Moturiki datum.

Mean sea level and model projected depth for the Deltares model were extrapolated for 2005 (baseline), 2025, 2055, and 2090 for each of 36 scenarios (3 positions: intertidal wetting and drying, edge of intertidal zone, subtidal platform; 4 RCPs (W/m^2): 2.6, 4.5, 6.0, 8.5; and 3 sediment delivery options (presumed baseline of 300 g/m^3; 20% increase; 20% decrease). Changes in depth at the Deltares intertidal wetting and drying position were assumed to apply to all depths classified as Saltmarsh and as Mangrove Upper (depths above 1 m below Moturiki datum). Changes in depth at the Deltares edge of intertidal zone position was applied to the Mangrove Lower classification (1 m to 2 m below Moturiki datum). Changes in depth at the Deltares subtidal platform site were assumed to apply to the Subtidal classification (depths >2 m below Moturiki datum).

Changes in depths were applied across all habitat classifications, and projected areas within each habitat type for 2025, 2055, and 2090 were calculated based on estimated change in bed level height from the Deltares model. Calculations of habitat classifications were based on 'suitable' habitat, recognising that even under current mangrove distributions, less than 100% of suitable habitat is colonised by mangroves. Mangrove mapped distributions suggest average percent cover of Mangrove Upper habitats of 62.2% (range: 21.0% – 84.1%), and Mangrove Lower habitats of 17.8% (range: 0.1% – 21.6%). Calculations of changes in saltmarsh habitat are conservative, and assumed that stopbanks or agricultural land-use prevents shoreward migration of saltmarsh in this area.

RESULTS

Firth of Thames sedimentation

The 3-D model scenarios used to determine plume and sediment dispersal in the Firth of Thames are based on the previous modelling study by Pritchard et al. (2015). We used a series of idealised scenarios with this model to determine sediment dispersal from the Waihou River, the main source of riverine freshwater and suspended sediment into the southern Firth. Results are shown in Figures 5 – 7, showing predicted maximum sediment deposition in the Firth of Thames that results from tide and wind driven forcing of the Waihou sediment plume. The results show that during calms the sediment sticks close to the source but during winds there is an increase in downwind (lateral and longitudinal) dispersion of the sediment plume, which, results in a larger more diffuse, sediment depositional footprint.

These Figures show that during a prevailing SW wind, sediment deposits up against the NE coast of the Firth; during a NE wind, sediment deposits up against the SW coast. Notably a lot of the deposition is in shallow water or intertidal regions close to the coast (Pritchard et al., 2015). The results from 3-D plume modelling imply that the Water Column Model projections would best represent the shallow water locations on the east or south coast of the Firth some distance from the Waihou river mouth (near field influence of river flows). These locations were shown by Pritchard et al. (2015) to be sediment deposition-centres being supplied by the Waihou plume.

The Water Column Model predicted inter-tidal, marginal and sub-tidal tidal platform development for the next 100 years are shown in Figures 8 – 10. The projections assume a sediment supply from the Waihou River plume and wind speeds are from the HadGEM2-ES MOHC (UK) climate model for all RCPs. The results are presented for the current situation in which a long-term open-water average suspended sediment concentration is taken as 300 g m^{-3}. [This is case (a) in these three figures.] Also shown are two other cases: (b) a reduction of 20% in open-water sediment concentration as may be experienced with some reforestation in contributing catchments, and (c) an increase 20% in open-water sediment concentration as may be experienced with substantial intensification of agriculture with little effort on adoption of Best Management Practices.

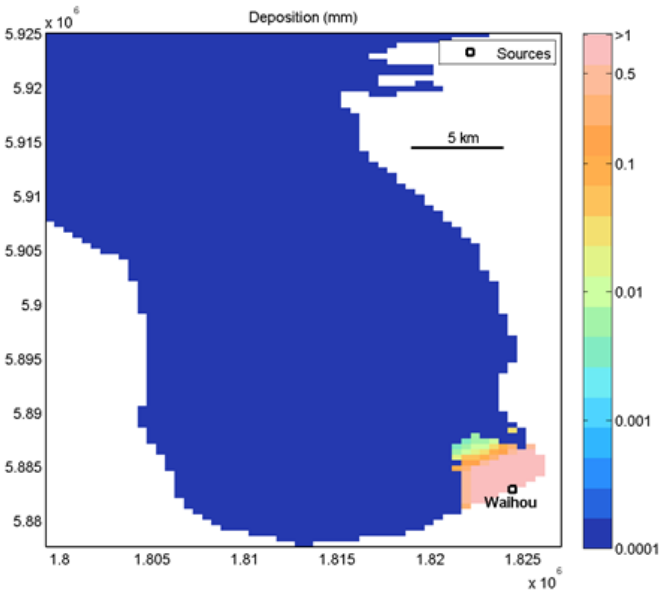

Figure 5 Predicted sediment deposition (mm) at the end of 30 day period in Firth of Thames under calm conditions.

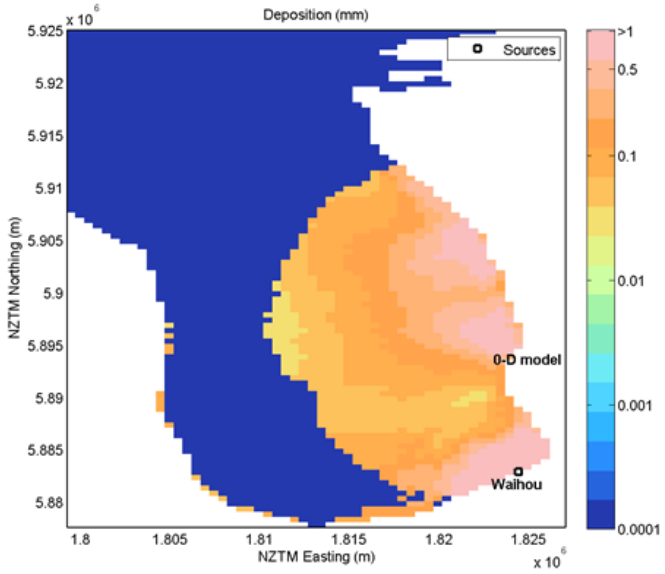

Figure 6 Predicted sediment deposition (mm) at the end of 30 day period in Firth of Thames under SW wind conditions ("0-D model" is a pseudonym for the 'Water Column Model'.)

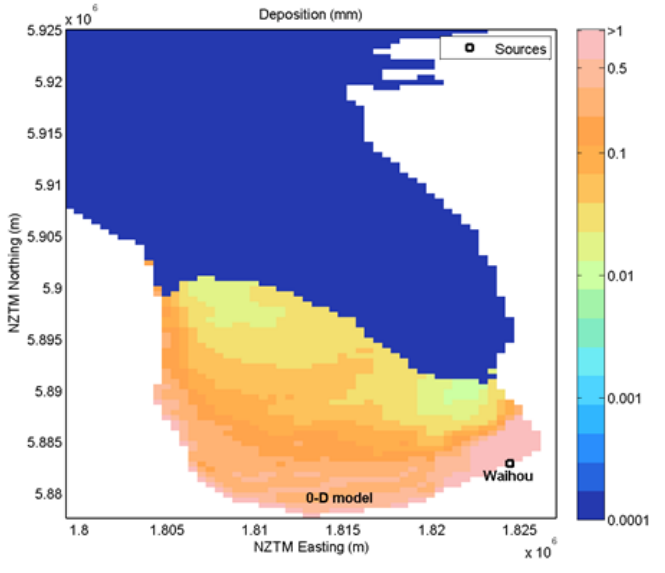

Figure 7 Predicted sediment deposition (mm) at the end of 30 day period in Firth of Thames under NE wind conditions. ("0-D model" is a pseudonym for the 'Water Column Model'.)

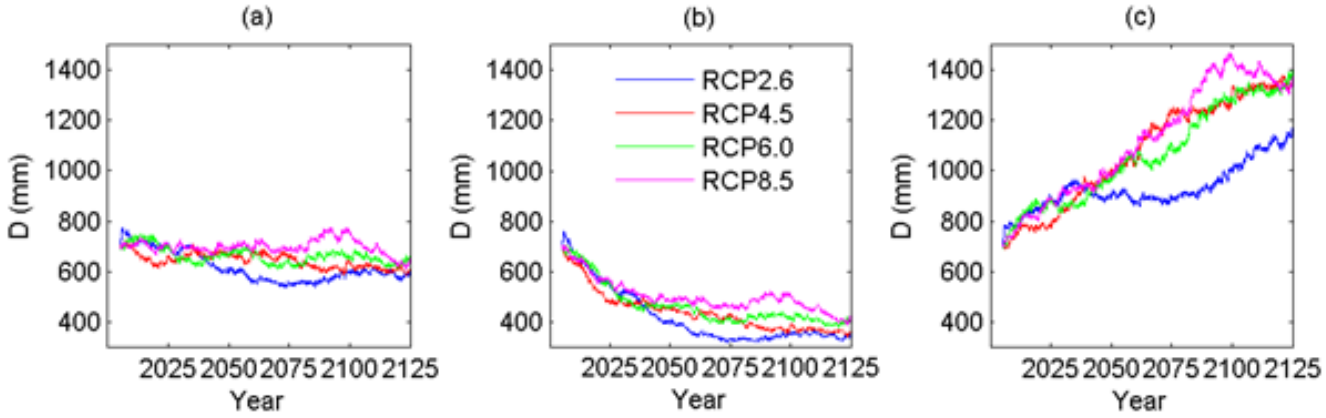

Figure 8 Predicted high-tide water depth by the Water Column Model for a drying and wetting intertidal platform (initial depth = 0.7 m, with tidal range = 1 m) based on four RCP-related wind scenarios and sea level rises (HadGEM2-ES model) and (a) constant 300 g m^{-3} sediment supply; (b) a 20 % increase in sediment supply; (c) a 20 % decrease in sediment supply.

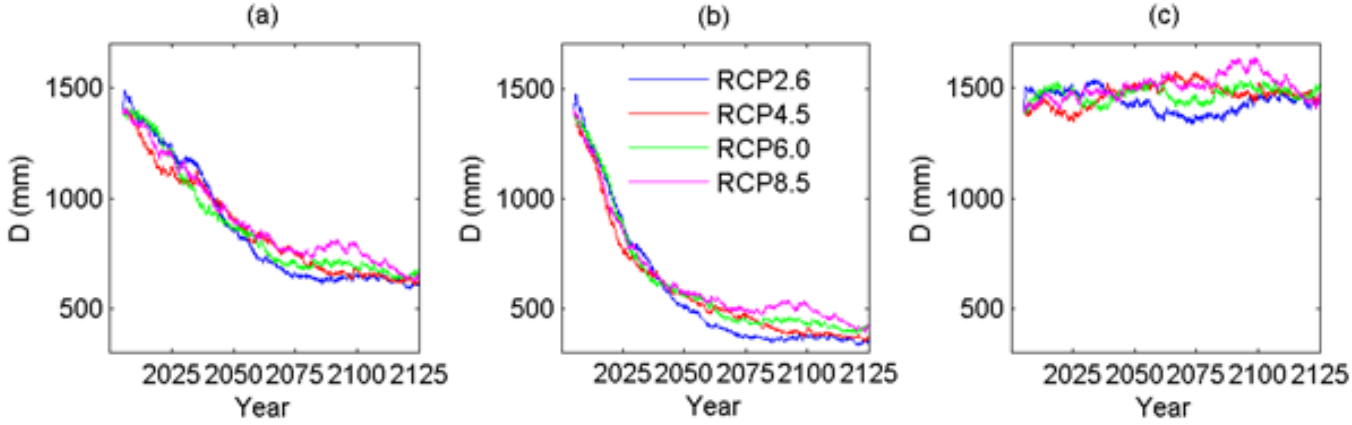

Figure 9 Predicted high-tide water depth by the Water Column Model for a marginal drying and wetting intertidal platform (initial depth = 1.5 m, with tidal range = 1 m) based on four RCP-related wind scenarios and sea level rises (HadGEM2-ES model) and (a) constant 300 g m^{-3} sediment supply; (b) a 20 % increase in sediment supply; (c) a 20 % decrease in sediment supply.

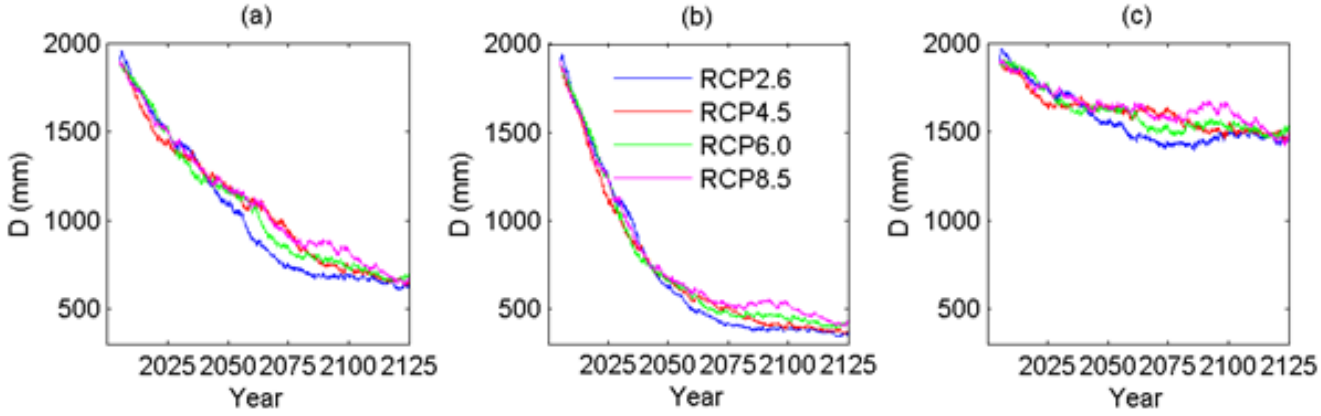

Figure 10 Predicted high-tide water depth by the Water Column Model for a subtidal (submerged) platform (initial depth = 2.0 m, with tidal range = 1 m) based on four RCP-related wind scenarios and sea level rises (HadGEM2-ES model) and (a) constant 300 g m^{-3} sediment supply; (b) a 20 % increase in sediment supply; (c) a p20 % decrease in sediment supply.

Results for another five GCMs are given in the Appendix, showing little inter-model variability with respect to the Firth modelling.

Mangrove distribution

Results for predicted changes in coastal habitat distributions under different sediment delivery and climate change scenarios suggest that sea level rise and sediment delivery interact to determine changes in coastal habitats with climate change. Note that neither shallow subsidence due to sedimentation and consolidation processes from de-watering of recent sediment deposits, nor deep subsidence due to tectonic/regional-scale geological processes, were included as potential factors in model projections. Swales et al. (2013) estimated rates of deep subsidence at ~0.008 m yr^{-1}, and Swales et al. (2015) suggest that shallow subsidence is a relatively minor component of surface elevation change at this location.

Comparison of RCPs with no change in sediment delivery (constant 300 g m^{-3} sediment supply) suggest that suitable mangrove habitat in the upper zone will increase >50%, and will double in the lower zone by 2090 under RCP 2.6, with sediment delivery contributing to long-term expansion mangrove habitat under conservative sea level rises associated with this RCP (Figure 11). RCP 4.5 gives similar changes in long-term mangrove expansion, though short-term increases in suitable mangrove habitat are larger in both upper and lower mangrove zones (Figure 12). RCP 6.0 is most similar to RCP 2.6 (Figure 13), whereas RCP 8.5 shows the smallest predicted increase in the mangrove upper zone (23.9% by 2090), and highest predicted increase in the mangrove lower zone (122.9% by 2090) (Figure 14).

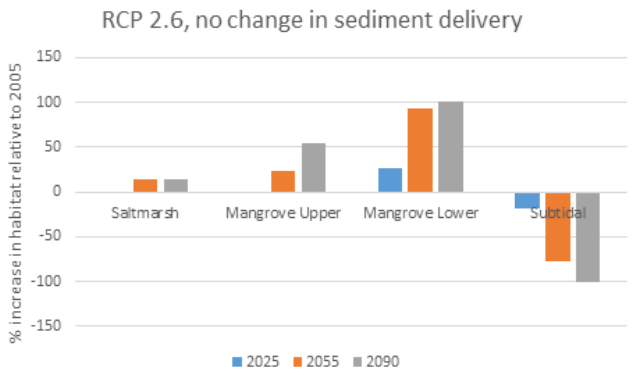

Figure 11 Predicted change in coastal habitats based on RCP 2.6 related-wind scenarios and sea level rises (HadGEM2-ES model) and a constant 300 g m^{-3} sediment supply.

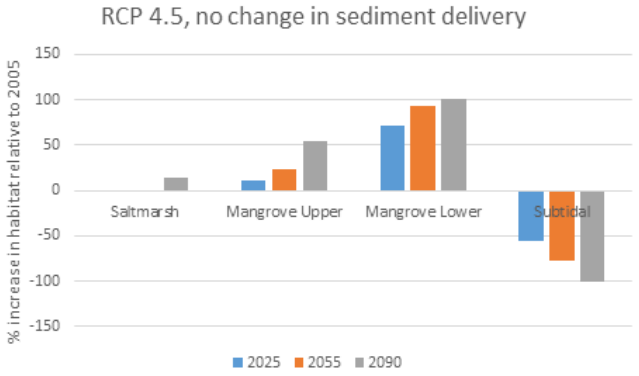

Figure 12 Predicted change in coastal habitats based on RCP 2.6 related-wind scenarios and sea level rises (HadGEM2-ES model) and a constant 300 g m^{-3} sediment supply.

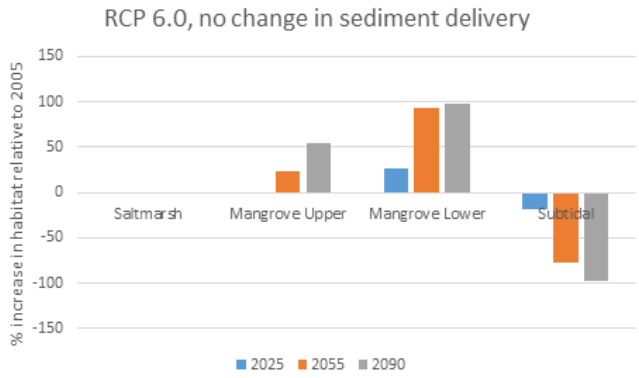

Figure 13 Predicted change in coastal habitats based on RCP 6.0 related-wind scenarios and sea level rises (HadGEM2-ES model) and a constant 300 g m^{-3} sediment supply.

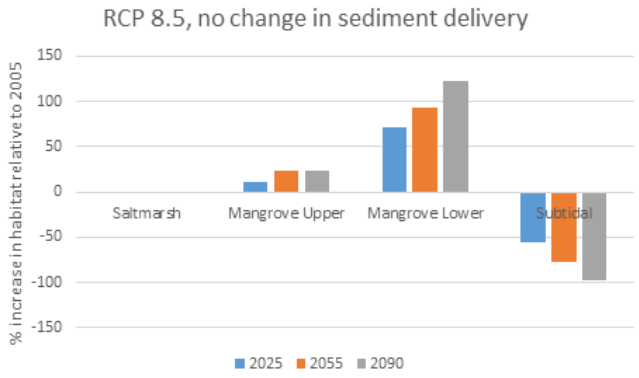

Figure 14 Predicted change in coastal habitats based on RCP 8.5 related-wind scenarios and sea level rises (HadGEM2-ES model) and a constant 300 g m^{-3} sediment supply.

Comparison of differences in sediment supply suggest significant reductions in sediment supply due to improved land-use management could reduce the amount of sediment delivery such that bed level height does not increase at rates compatible with sea level rise, resulting in decreases of up to 34.1% in the upper mangrove zone, and corresponding increase of up to 53.8% in the mangrove lower zone under RCP 6.0 as these depths shift from upper to lower mangrove zones with sea level rise (Figure 15). In contrast, increasing sediment supply even during relatively high sea level

rises associated with RCP 6.0 results in expansion of suitable mangrove habitat, with 81.1% and 80.2% increases predicted by 2090 for mangrove upper and lower zones, respectively (Figure 16).

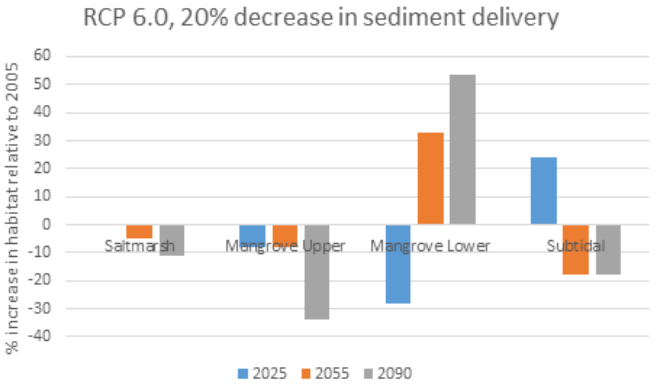

Figure 15 Predicted change in coastal habitats based on RCP 6.0 related-wind scenarios and sea level rises (HadGEM2-ES model) and 20% decrease in sediment supply.

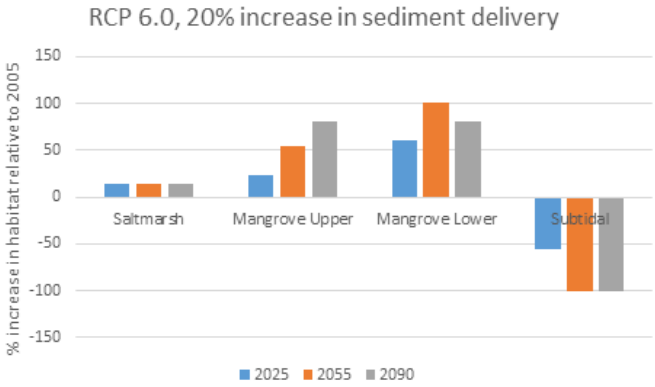

Figure 16 Predicted change in coastal habitats based on RCP 6.0 related-wind scenarios and sea level rises (HadGEM2-ES model) and 20%, increase in sediment supply.

Waihou and Piako River flows

TopNet was run continuously from 1971-2100, with the spin-up period 1971 excluded from the analysis. The simulation results comprise hourly time-series of several hydrological variables for each computational sub-catchment, and for each of the six GCMs and four RCPs considered. To manage the output data size, only river flows information was preserved; all the other state variables and fluxes are available on demand once regenerated. As a further data management step, statistics were derived from the three periods spanning 2015-2035 ('early-century'), 2036 to 2055 ('mid-century') and 2086 to 2099 ('late-century'), as well as the 'baseline' period spanning 1986 to 2005. The results for the six GCMs were combined into a multi-model median (as hydrological processes tend to be of non-Gaussian nature), and the results of the RCPs were kept separate.

In summary, the median change (across all GCMs) of the mean annual flow for the Waihou and Piako catchments, for all RCPs and for all three time slices (compared with the baseline period), is relatively small (around ±5%), which is consistent with the median projected precipitation changes for this region. However, there is a lot of variation between the GCMs (with changes to annual flows from individual models in the range of ±20%; again representing the variation in precipitation projections), suggesting the level of uncertainty in the median change is quite high.

Comparing seasonal flows for RCP 8.5, the median change in mean winter and summer river flows for the Waihou and Piako catchments is predominantly negative and in the range of 10 – 50% (the high end of this range is in late-century). On the other hand, in spring and autumn, mean river flows are expected to increase by the end of the century by a similar range (10 – 50%).

As with the changes to mean annual flow, there is significant variation in the projected changes to seasonal flows for these catchments across the six GCMs, therefore caution should be exercised when interpreting these results. The approach we take when investigating changes in saltwater intrusion in the Waihou under different mean annual low flows (see next Section) is a sensitivity analysis using possible changes of ±10%. Given the uncertainty in the projected changes in river flows for this region, this is a preferred approach. Such an assessment could be repeated for other potential flow changes.

Waihou salinity intrusion and river flooding

Salinity intrusion

The modelling effort was separated into two components covering changes in saline intrusion and extreme water levels along the river. The first section discusses the salinity distribution and changes in the lower Waihou River under four SLR scenarios (0.3, 0.5, 0.7 and 1 m) for a relevant mean annual summer low flow, while all other conditions remain unchanged. These SLR scenarios cover the range of plausible values for the four RCPs. Results are displayed on Figure 17.

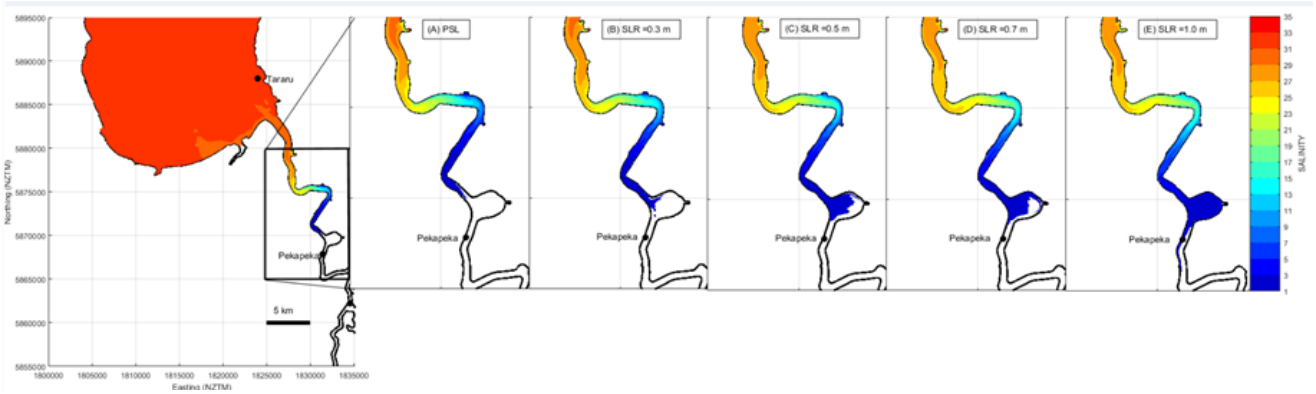

Figure 17 Distributions of bottom salinity for scenarios with mean annual low flows. Minimum bottom water salinity contour is 0.5 (psu).

These results show that the flood-tide saline intrusion would intrude about 5 km farther upstream in the Waihou River for a 1 metre SLR.

The mean annual low flow was inflated and reduced by up to 10% to test whether the position of the saline intrusion was sensitive to changes in low flow. (We consider that 10% conservatively encompasses the likely range of potential climate change effects on low flows.) The modelled scenarios show that this range of change in low flow would not have any discernible effect on the position of the 0.5 (psu) salinity contour in the lower Waihou River. In the Waihou River the most significant driver for the upstream position of the salt wedge is the level of the sea.

Figure 28 (Appendix) presents the variability in projected intrusion lengths by the six GCMs.

River flooding

The second component looks at the effect a SLR of 0.5 or 1 m could have on the extreme water levels in the Waihou River and changes in where the maximum occurs along the reach. Results are displayed on Figure 18. Main results, excluding storm tide considerations, show that for the upper Waihou River (50 km upstream from mouth and above) the impact of SLR will be minimal, because this zone of the river is dominated by the river flow.

The top panel (A) in Figure 18 illustrates the impact of SLR on current mean annual low flows. The base low flow with 0.5 m SLR (red line) shows the that the tidal limit in the Waihou River would move 6 km upstream (56 km from the mouth) from Tirohia tide gauge (current tidal limit). The base low flow with 1 m of SLR (black line) scenario suggests the tidal limit will move a further 3 km upstream. The flood ARI modelling illustrated in the other five panels shows that water levels in the Waihou River between Puke Bridge and 50 km upstream from the mouth can expect smaller, more frequent nuisance floods to be influenced by SLR, but as the river flood increases in size to over 20-year ARI (panel D), the upstream effect of SLR rise is washed out by the river flood (regardless of the magnitude of SLR up to 1 m). The largest impact of SLR and <20-year ARI flood interaction will occur in the lower Waihou River between Pekapeka and Puke Bridge. Sea-level rise impacts on total water levels diminish with distance upstream from the Waihou River mouth –for example, the 10-year ARI flood profiles. A 1 m sea-level rise by the year 2100 or 2120 could result in a 0.5 m increase in total flood level at Pekapeka and a 0.1 to 0.2 m increase in flood level at Puke Bridge, compared to present-day for the same flood event. Upstream from Puke Bridge, sea-level rise would have a negligible effect on total flood levels.

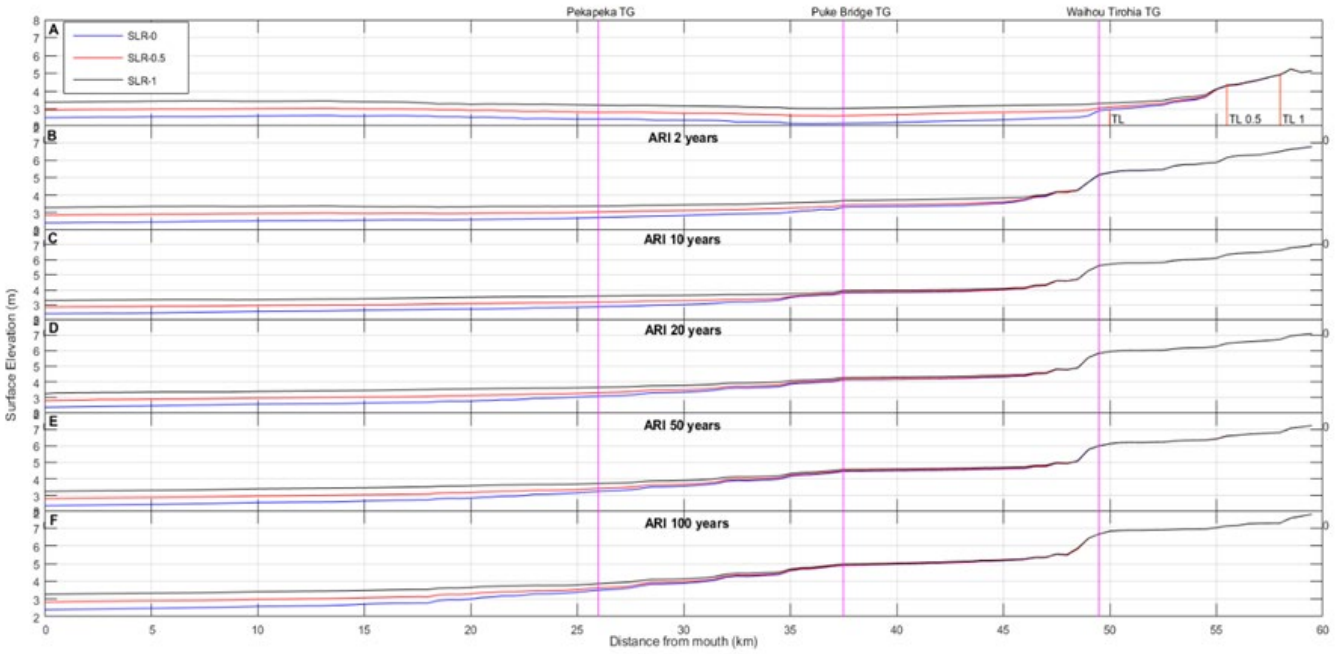

Figure 18 Maximum water levels extracted from a thalweg transect of the Waihou River. The blue lines represent present day sea level; red lines represent a 0.5 m SLR scenario and the black lines represent a 1 m SLR scenario. Pink vertical lines indicate the location of water level recorders. The top panel is for present-day mean annual low flows. The other three panels are for increasing Average Return Intervals, indicated by the ARI headers.

KEY FINDINGS AND IMPLICATIONS

Drying and wetting in the Firth

The combinations of 3D and 'Water Column Model' models in the Firth sedimentation part of this case study is novel, in that the Water Column Model is in many respects new, especially in the manner it can handle drying and wetting. The 3D model results show that the Water Column Model would best represent the shallow water locations on the NE or SW coast, away from the Waihou River mouth.

Accordingly, Figures 8 –10 show projections for three initial high-tide water depths: 0.7 m, 1.5 m and 2 m. Part (a) of those three figures show that under a scenario with a common open-water sediment concentration averaging 300 g m^{-3} the water depths over time are relatively independent of the RCPs. In other words, as the sea level rises the bed level tends to rise similarly. Never-the-less, as expected the greatest predicted depths occur for RCP 8.5, for which SLR is most extreme.

Figure 8(a) indicates that there is an equilibrium in that the high-tide depth is relatively unchanged over time, and substantial drying occurs below mid ebb tide (the tidal range is 1 m, so drying would occur at some part of the tidal cycle when the predicted high tide depth is less than 1 m). For greater initial depths [1.5 m and 2 m, Figure 9(a) and Figure 10(a)] there is a reduction in high-tide depth over time, again with the RCP 8.5 being the least affected. There is no drying and wetting in the early years. Nevertheless, after 100 years roughly the same equilibrium point will have been reached as occurs for the shallowest case (0.7 m at high tide) and a similar drying and wetting pattern would emerge. The (b) component of the three figures (open-water sediment concentration = 360 g m^{-3}) indicates that there will be rather more drying as the years go by and even more than for the 300 g m^{-3} case (a). In contrast the (c) component of these results (open-water sediment concentration = 240 g m^{-3}) show an increase away from any drying reached an equilibrium high-tide concentration depth of about 1.5 m.

The striking result is that the Firth water depth distribution depends not so much on RCP-related sea-level rise, as it does on the sediment delivery to the Firth from land practices and associated sediment runoff.

Mangrove distribution in the Firth

Model projections suggest that sediment supply and sea level rise both drive changes in suitable mangrove habitat. In most scenarios with current or increasing sediment supply, suitable mangrove habitat is maintained or expanded, and sediment supply is sufficient to maintain mangrove distributions through the building of bed level height due to sediment deposition. In contrast, for scenarios with reduced sediment supply, large decreases are predicted for mangrove upper zones as sediment supply is not sufficient to maintain mangrove distributions in the face of sea level rise.

Land-use policies and practice need to be cognisant of the primary role played by sediment runoff on the evolution of bathymetry and water depth in the Firth of Thames, as exemplified by model projections over the next 100 years. Under some scenarios, sea level rise and sediment supply show signs of being in equilibrium, whereas other scenarios suggest enhanced land-use and reduced sediment supply would have downstream impacts on long-term distributional changes in mangrove habitats.

River flows

Projected changes in river flows for the Waihou and Piako catchments are strongly linked to projected changes in precipitation across the region. In general, the median change in the annual mean flow is relatively small, with generally negative changes in winter and summer (decreased mean flow), and positive changes in spring and autumn (increased mean flow). Such changes will have important implications for water extraction and the maintenance of minimum flows (particularly in summer).

It must be noted however, that when comparing projections in river flows derived from individual GCMs and RCPs, there are very large differences (in the general trend and the spatial pattern) between different TopNet model runs. These differences have been traced to the large inter-GCM differences in the precipitation projections for this region. In this situation of large uncertainty, we feel it is more appropriate when performing impact assessments not to dynamically link the flow projections to the impact models. Instead, we have chosen a conservative range of possible future flows within the bounds of the TopNet projections (e.g. ±10%) and have investigated the sensitivity of the impacts to this range. Should there be impacts that are sensitive to this range

of possible changes, then risk-based adaptation measures that can be monitored and modified over time are advised.

Salinity intrusion and flooding

Coastal zones and adjoining lowland freshwater systems are particularly vulnerable to climate change effects, particularly from sea-level rise. By the end of this century or early next century, we could expect to see upwards of a 1 m rise in sea level, particularly if instabilities develop in the polar ice sheets and if global emissions push global average temperatures beyond 2°C above pre-industrial levels (Hannah & Bell 2012; Golledge et al. 2015).

Humans and aquatic fauna and plants all rely on present supplies of fresh water in lowland rivers, but these modelling simulations demonstrate that SLR will progressively lead to salinization of these freshwater resources (punctuated only by flood events). This is because permanent SLR leads to increase in saline-water energy head at the ocean boundary of the river system, which sustains sea water intrusion further upstream (Werner and Simmons 2009). Salt water intrusion is an important phenomenon in coastal zones, and can create a serious problem to people and communities due to the need for fresh water for potable water services, agriculture and industry (Zhang, Savenije et al. 2011). Salt water may also infiltrate coastal aquifers and movement of saline water into ground water resources in coastal regions, resulting in decreasing water quality (Bashar and Hossain 2006; Werner and Simmons 2009) and effects on flora and fauna and conservation management (Kettles & Bell, 2016).

For drinking water, the maximum allowable concentration is 250 mg/L (or ~0.5 psu) for chloride (MoH 2008). For the modelling undertaken in this case study we used the 0.5 isohaline as the 'cutoff' limit for defining the upstream limit of saline intrusion. The modelling undertaken in the Waihou River shows that isohalines will move progressively upstream as the SLR increases, with the maximum extent about a further 5 km upstream for a 1 m SLR (see Figure 17). Future resource-management planning for the lower Waihou River, including water resource allocation, will need to assess and eventually limit freshwater extraction below Puke Bridge or more precisely 27 km from the mouth. In the Waihou River the most significant driver for the position of the salt wedge is the mean level of the sea.

The TELEMAC3D simulated model results were also used to determine the possible effects of SLR on total water levels in the Waihou River system during flood events. Flooding in the lower Waihou River will be affected by a rise in sea level, but for the upper Waihou River (50 km and above) the simulations show the impact of SLR will peter out because this zone is dominated by the river flow. From Waihou River to Puke Bridge (35 – 50 km from mouth), smaller, nuisance floods on the back of higher SLR, will increase total flood water levels, but as river flood events exceed a 20-year ARI, the effect of SLR rise is washed out by the flood. The largest impact of SLR and flood interaction will occur in the lower Waihou River between Pekapeka and Puke Bridge, with up to a 0.5 m increase in combined flood level at Pekapeka for a 1 m SLR.

SCENARIOS, TAKING ACCOUNT OF ECONOMICS AND PUBLIC POLICY

The architecture for New Zealand scenarios adopts two global elements from a global scenario toolkit (Ebi et al., 2013) plus one national-scale element. These are global RCPs, global Shared Socio-economic Pathways (SSPs) and New Zealand-specific Shared climate Policy Assumptions (SPANZ) (see the CCII RA5 Synthesis Report for more details). The last item is required if, for example, New Zealand's population declines and the country embarks on a programme of reforestation, whereas the rest of the world adopts much more intensive agricultural practices.

Shared socio-economic pathways (SSP)

Unlike earlier assessments, scenarios for climate change decouple the climate model outputs, expressed through RCPs, from their socio-economic drivers, expressed through the concept of SSPs—Shared socio-economic pathways describe plausible trends in the evolution of society and global economy. van Vuuren and Carter (2013) introduced a framework to illustrate combinations of RCPs and SSPs.

Shared Policy Assumptions for New Zealand (SPANZ)

The Shared climate Policy Assumptions (SPAs) are specific to New Zealand. SPAs describe potential climate change mitigation and/or adaptation policies not specified in the SSPs. They provide a third axis to the scenario matrix and allow national-level development choices that may reinforce global trends or actively go against them.

Elements of scenario analysis

To help assess these, O'Neill et al. (2013) suggested outlining several elements that are relevant for defining both challenges to mitigation and adaptation, as shown in Table 2.

Scenario modelling

We applied several agricultural yield, economic and land use models to the Waihou catchment to conduct the RCP/SSP/SPANZ scenario analysis. The series of models (see section 1.3) was available to quantify some elements of resources (water and land), demographics, economic development (trends in commodity prices, primary production changes, land use suitability and land-use change patterns) and environmental factors (erosion and GHG emissions). Details on each model are provided in the Appendix.

Integrated assessment

One of the objectives for the CCII project was to provide an integrated view of how the different parts of the landscape interact with each other, using the outputs from the modelling approach as much as possible. To achieve this, models were linked to each other and tested through future scenarios to better understand interactions and feedbacks. Research Aim 5 provided the scenarios that were to be tested (see CCII RA5 synthesis report).

To help assess plausible scenarios, the elements in Table 2 (O'Neill et al., 2013) were evaluated quantitatively via modelling where possible, and complemented with narratives from the CCII research team.

Categories	**Elements**
Demographics	Total population and age structure, urban vs. rural populations, and urban forms
Economic Development	Global and regional GDP, trends in productivity, sectoral structure of national economies (share of agricultural land)
Environmental factors	Air, water, soil quality, ecosystem functioning
Resources	Fossil fuel resources and renewable energy potentials fresh water, land.
Welfare	Human development, educational attainment, health.
Institutions and governance	Existence, type and effectiveness of national/regional/global institutions
Technological Development	Type (e.g. slow, rapid, transformational) and direction (e.g. environmental, efficiency, productivity) of progress
Broader societal factors	Attitudes to the environment/sustainability/equity and world views, life styles, societal tension and conflict levels
Policies	Non-climate policies

Table 2 Elements of scenario analysis (adapted from O'Neill et al., 2013).

Each element from the Table was assessed on the basis of an example scenario. For this case study, we tested the following four combinations:

1. RCP8.5/SSP3/SPA-A
2. RCP6.0/SSP5/SPA-D
3. RCP4.5/SSP5/SPA-F
4. RCP2.6/SSP5/SPA-B

More details on each scenario are provided in Table 3.

The models operate at different scales (sector-based scale and landscape scale) and have as inputs either the RCP scenario only (primary production, wetlands) or a combination of RCP and SSP assumptions (for example the land-use change models). We assessed each scenario from 2015 to 2100 using assumptions specific to each RCP/SSP/SPA combination. Estimated impacts are generally presented at mid and end-century points.

Table 3 Scenario description.

ID	RCP	SSP	SPANZ	Scenario Sketch	Coastal case study-specific Assumptions
Base	None	None	None	Baseline. Land use, commodity prices, technology, and agriculture and forestry yields are all based on 2015 estimates. No climate change (RCP) impacts. No SSP impacts.	None
8.5/3/A	Very high emissions (8.5 W/m^2)	SSP 3 Fragmented World	A: With NZ lagging relative to global efforts to mitigate, nationally there is only incremental and reactive adaptation on a piecemeal basis.	Unspecific Pacific. An increasingly highly populated world, with break-down of open trade and security, regional crises and financial instability. New Zealand is part of a Pacific backwater that is sliding downwards economically, with refugees from Pacific Islands with military conflicts between Australia and Indonesia. Impacts of climate change on NZ are dealt with as and when they occur with local solutions generating problems due to short-term decision-making. Free trade is with volatile partners who require constant attention and accept their prices to protect trade routes and access with military force. A severely resource-constrained world neither cares nor can afford the luxury of environmental goals and, bar a few militant voices, there is little premium on such values. Investment in technology is very short-term and environmental conservation is a low government priority.	Sediment increases by 20% over baseline
6/5/D	Stabilization (6 W/m^2)	SSP 5 Conventional Development (fossil powered growth)	D: NZ lagging global mitigation which is too little, too late globally for energy security, health and efficiency gains. Adaptation strategy is to maximise economic opportunity.	Homo Economicus. Global mitigation is largely only what provides direct co-benefits for health, energy security and economic efficiency given rising resource costs. NZ is using oil and gas fields and renewables as the lowest cost energy mix, the bulk of which is processed in the deep ocean so that GHG credits are attributed to the purchaser and not to NZ. There are no efforts to reduce GHG emissions specifically and certainly not from agriculture which continues as a major export earner. Impacts and risks from climate change are taken seriously solely for their economic implications including biosecurity for primary production. Assets are mostly protected by additional infrastructure, but strategic land-use decisions are made with a medium-term economic focus through market mechanisms. High discount rates are a major driver for government expenditure and environmental conservation is a low government priority.	Sediment decreases by 20% relative to baseline
4.5/5/F	Intermediate stabilization (4.5 W/m^2)	SSP 5 Conventional Development (fossil powered growth)	F: NZ ahead of increasingly stringent global efforts to mitigate, and strategic approach to adaptation to maximise not just economic opportunities but to achieve sustainability across three pillars	Clean Leader. Global emissions are actively being reduced through sharing more efficient conventional technologies and ensuring mitigation is achieved where most cost-effective. Countries continue to argue for economically important sectors to be exempt from emissions obligations. NZ is developing innovative low-cost mitigation opportunities and actively trading those for economic gain to the highest bidder. Factory-based GE farming is unregulated but restricted to offshore islands. Strategic land-use decisions are made with a view to maximising economic growth in a warming and carbon-constrained world. When it comes to balancing trade-offs in adaptation responses, economic concerns win over environmental or societal equity concerns. NZ leads global practice in free-market emissions trading. Variable discount rates are explored in NZ as a means of creating change which is attracting global profile for NZ goods and services with environmental conservation a strong government-business partnership.	Sediment decreases by 20% relative to baseline
2.6/5/B	Low mitigation (2.6 W/m^2)	SSP 5 Conventional Development (fossil powered growth Conventional Development (fossil powered growth)	B: NZ complies with very stringent global efforts to mitigate, reactive and incremental approach to adaptation with focus on economic gains	Techno-garden. NZ fully engages in stringent global efforts to reduce emissions and meets a large part of its obligations internationally through emissions trading since it proves more lucrative to grow low-emissions livestock products and use some of the money to pay for credits. This is important since international regulations and effective branding schemes exist to promote consumer choice of low-emissions products. Responses to climate change impacts through most cost-effective way consistent with maximising economic returns. Highly regulated GE-led production, off-shore oil extraction and processing plus low-impact nuclear technologies enable NZ to dominate premium niche value markets. Communities are increasingly controlled by high-tech protection systems except in low-value neighbourhoods considered not worth protecting. Low discount rates used to stimulate change. Environmental conservation a high government priority.	Sediment decreases by 20% relative to baseline

Scenario estimates

Primary production

The yield models estimated that each RCP and GCM is likely to have a varying effect on agricultural commodity yields. Mean impacts relative to the 2015 baseline yields for all 4 RCPs are listed in Table 4. Note that the figure for each RCP is also based on the average impacts measured over all 6 GCMs used for the case study. Thus the figures here can be interpreted as an average of an average. The key finding from this aspect of the analysis is that timber yields in the catchment are expected to increase significantly more than pastoral yields, regardless of the RCP. Average yields for all agricultural commodities are expected to increase in nearly all cases, with the one exception being sheep & beef outputs under the RCP 8.5 case. In addition, standard deviation of yield changes over the Waihou and Piako catchments is estimated to increase across the RCPs, indicating that the range of impacts is largest under RCP 8.5.

Table 4 Estimated yield impacts for CCII Coastal Case Study, catchment average (2015 baseline = 1).

Output	Metric	RCP 2.6	RCP 4.5	RCP 6.0	RCP 8.5
2050					
Milk	Mean	1.035	1.030	1.025	1.020
	StDev	0.003	0.007	0.012	0.019
Meat/Wool	Mean	1.024	1.012	1.002	0.991
	StDev	0.002	0.004	0.007	0.011
Timber	Mean	1.087	1.080	1.101	1.120
	StDev	0.018	0.024	0.019	0.024
2100					
Milk	Mean	1.033	1.050	1.065	1.082
	StDev	0.004	0.006	0.012	0.018
Meat/Wool	Mean	1.025	1.039	1.051	1.065
	StDev	0.002	0.004	0.008	0.013
Timber	Mean	1.073	1.148	1.210	1.245
	StDev	0.017	0.030	0.032	0.041

Commodity and GHG Prices

For this analysis CliMAT-DGE was 'tuned' to closely match projections published in the IIASA RCP and SSP databases. In this case, we focused on Global and New Zealand population, gross domestic product (GDP), and GHG emissions for the various scenario combinations. Doing so facilitated the estimation of global and domestic commodity prices that could be used as inputs to other modelling used in this study, namely for the NZFARM and LURNZ Models. This scenario estimated that the largest changes in commodity prices would occur for oil (not shown), sheep and beef products (meat and wool), forest products (timber), and dairy products (milk). We find that pastoral commodities are estimated to see dramatic price increases over time, not only due to increases in demand associated with global population growth, but also as a result of national and global climate change reduction policies that place a price on GHG emissions from all sectors of the economy, including agriculture and livestock.

CliMAT-DGE estimated that GHG prices were required for all but the RCP8.5/SSP3 scenario in order to meet the New Zealand GHG emissions targets specified for each scenario. Prices are relatively modest for RCP6.0/SSP5 scenario as NZ still has a relatively high emissions trajectory. However, large GHG prices are required in the second half of the century under the RCP4.5/SSP5 and RCP2.6/SSP5 scenarios, which require that GHG emissions are reduced by 50% or more relative to the baseline (Figure 19).

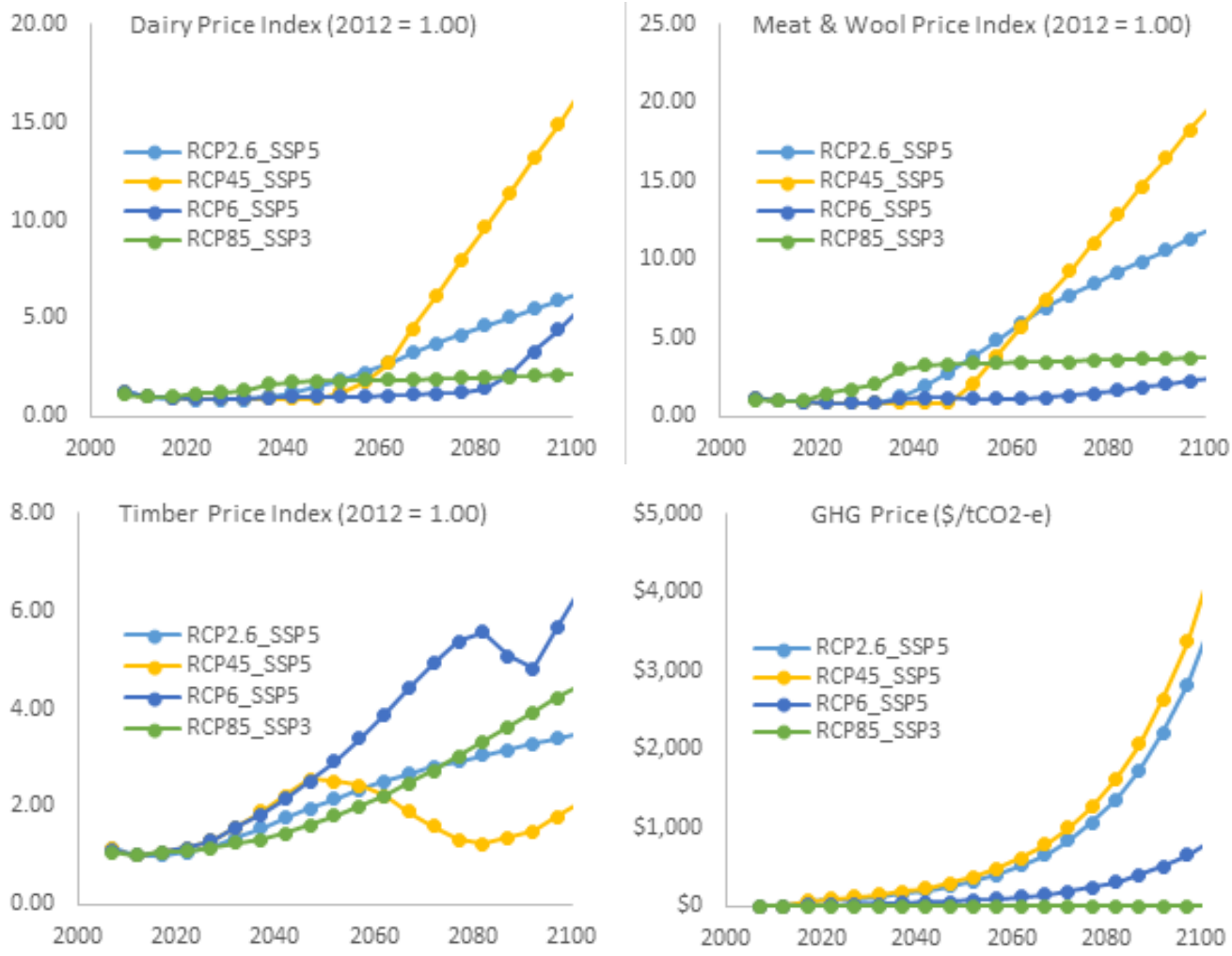

Figure 19 Scenario Price Estimates, based on CliMAT-DGE model.

Land use and environmental outputs

This component of the scenario analysis used NZFARM to estimate land-use change and resulting impacts on land-based environmental outputs. Some of the key 2015 baseline (no climate change) estimates are shown spatially in Figure 20. Apparent in the figure is that the dominant land uses in the catchment are dairy and native bush, followed by sheep & beef and plantation forestry. As a result, there is a clear divide in the source of net farm revenue, soil erosion, and GHG emissions that generally flows through the middle of the catchment.

For the scenario analysis, NZFARM estimated that the greatest change in land use over the different scenarios is estimated to be between forest plantations, sheep & beef (S&B) farms, and other (e.g., fallow) land use (Figure 21). This is driven not only by changes in yields and commodity prices, but also by the constraint on whether sediment was expected to increase or decrease based on the scenario. In the case where sediment increased (RCP8.5/SSP3 and RCP6.0/SSP5), there is a shift from forestry and other pastoral land to sheep & beef, which tends to have high erosion rates, particularly on moderate and steep sloped areas of that catchment that were originally

forested. In the scenarios where sedimentation was targeted to decrease by 20%, there is an estimated shift in dairy and sheep & beef to forestry, scrub, and fallow land.

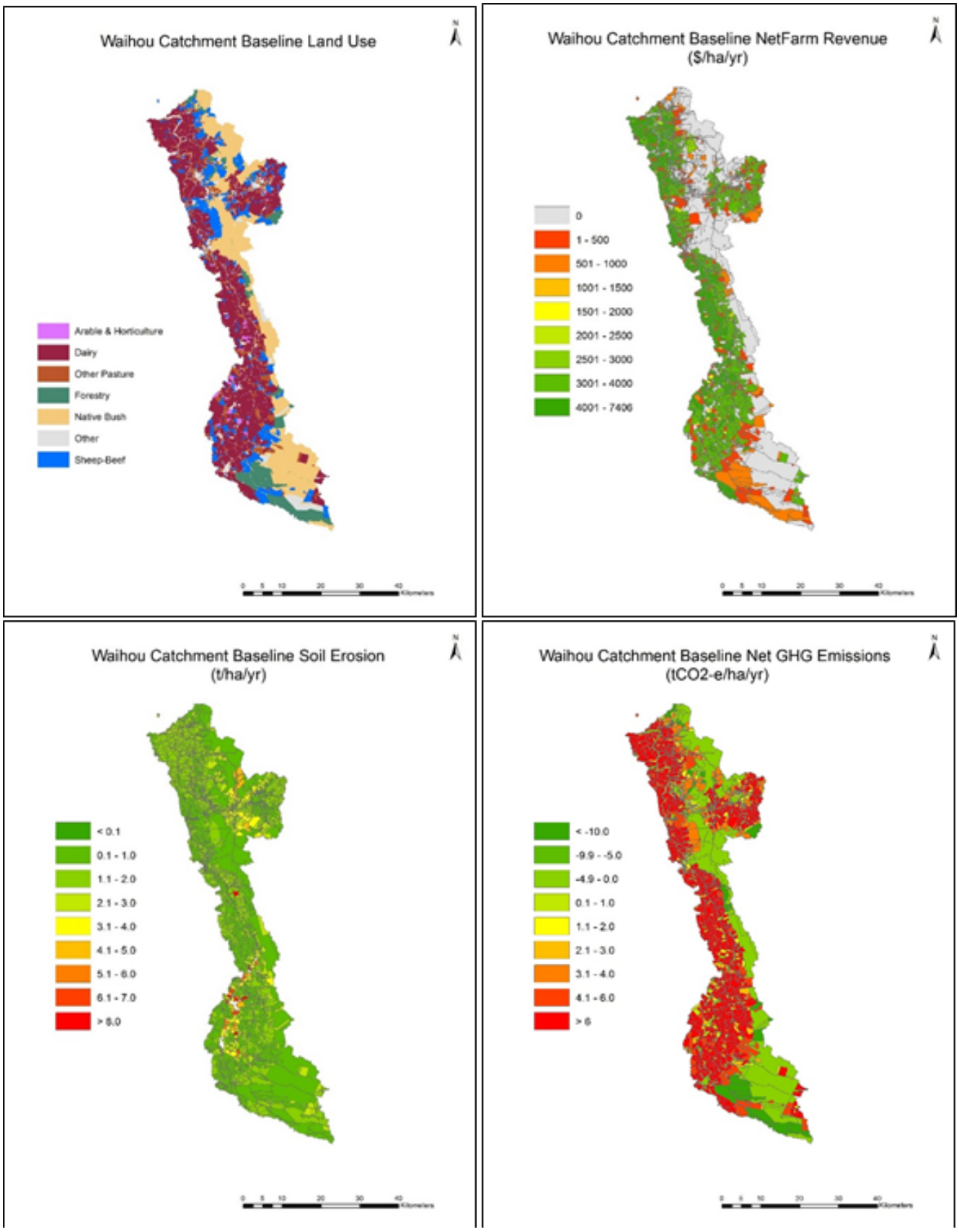

Figure 20 NZFARM baseline land use, net farm returns, soil erosion, and GHG emissions.

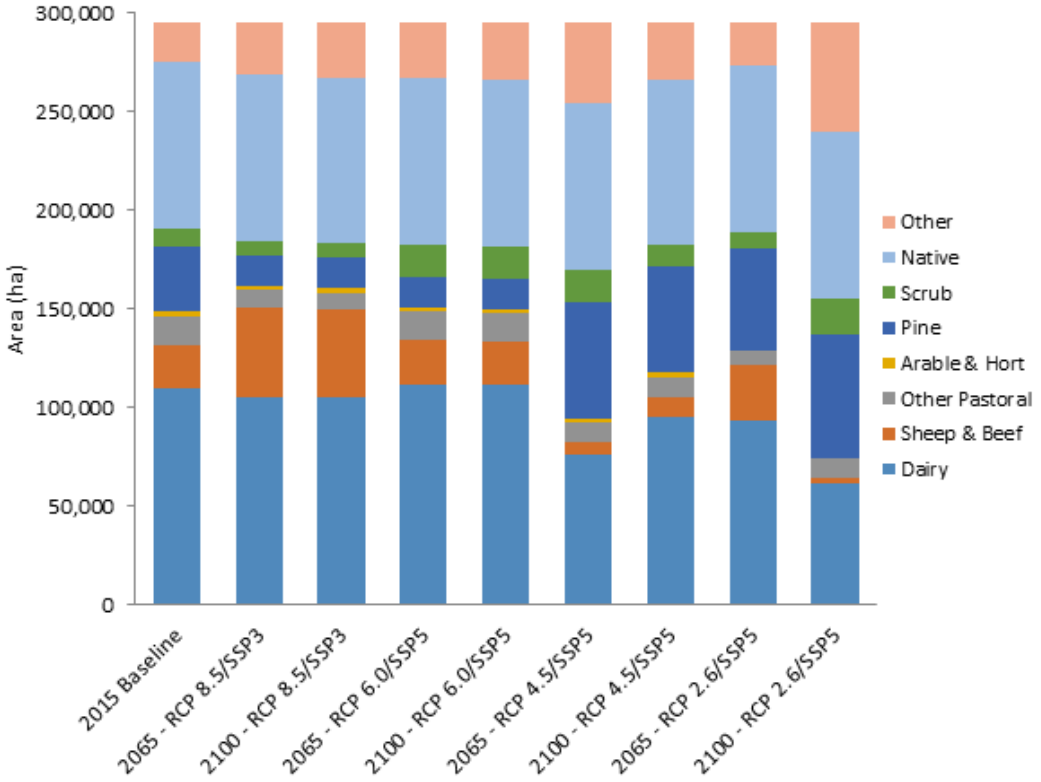

Figure 21 NZFARM catchment-wide land use estimates, by scenario.

The estimated impacts on land use in the catchment have a flow on effect on annual environmental outputs and farm earnings (Table 5). For example, the RCP 8.5/ SSP 3 and RCP 6.0/ SSP 5 scenarios that specify a 20% increase in soil erosion (and resulting sedimentation) leads to an expansion of pastoral enterprises and deforestation, which results in greater GHG emissions and P loss within the Waihou as well. On the other hand, the more environmentally-minded scenarios (RCP 4.5/SSP 5 and RCP 2.6/SSP 5) are estimated to not only decrease sediment by 20% relative to the 2015 baseline, but also reduce gross and net GHGs and nutrients. In addition, there is wide variance in the net farm returns in the catchment, which is influenced by the large variation in commodity and GHG prices across scenarios more than anything else. Further analysis has indicated that all of the environmental and economic impacts estimated in NZFARM are more heavily influenced by the SSP/SPA assumption than the climate change yield impacts as commodity prices, GHG prices, and environmental constraints are all more significant than the 5-10% change in primary production over the next century.

Table 5 NZFARM Key estimates for CCII Coastal Case Study.

Scenario	Year	Net Farm Revenue ($)	Gross GHG Emissions (t)	Total C Sequest (t)^	Net GHG Emissions (t)*	N Leaching (t)	P Loss (t)	Soil Erosion (t)
2015 Baseline	2015	491.4	849,220	-832,289	16,931	4,007	123	219,898
% change from baseline								
RCP 8.5/SSP3	2065	162%	20%	-43%	3165%	0%	17%	20%
RCP 8.5/SSP3	2100	266%	20%	-43%	3110%	0%	15%	20%
RCP 6.0/SSP5	2065	18%	13%	-39%	2597%	-1%	2%	20%
RCP 6.0/SSP5	2100	9%	13%	-39%	2570%	-1%	1%	20%
RCP 4.5/SSP5	2065	106%	-25%	76%	-4989%	-28%	-40%	-20%
RCP 4.5/SSP5	2100	2683%	-8%	57%	-3161%	-13%	-24%	-20%
RCP 2.6/SSP5	2065	178%	1%	52%	-2507%	-12%	-9%	-20%
RCP 2.6/SSP5	2100	1238%	-41%	85%	-6206%	-41%	-53%	-20%

^ Currently excludes change in carbon sequestration from mangroves.
* Negative figure indicates that total emissions less sequestration in catchment go from net source to sink

SUMMARY AND CONCLUDING REMARKS

This report draws attention to the interplay between global markets, New Zealand's policy choices (SPANZ) landuse change and the amount of sediment entering the rivers flowing into the Firth of Thames. Both the physical environment and the ecology of the Firth, will be shaped by the relationship between sediment supply and sea level rise. In turn, changes within the Firth will affect what is valued by local communities, iwi/hapu and stakeholders (Figure 1). In particular, important estuarine habitats like intertidal flats, shellfish and flounder habitat.

Changes in the flow regime and increased salinity intrusion up the Waihou River may have implications for local water takes (e.g., irrigation, stock or potable water) and river ecology. This will potentially affect access to localise water sources and community, iwi/hapu and stakeholders in–stream values.

An appreciation of these interrelated impacts and their implications begins to provide insights into the nature of the challenges and choices a changing climate could create within the Firth of Thames and surrounding catchments. Further investigations based on the multitude of research needs outlined in this report will further elucidate the impacts and implications of climate change in this case study area, and the methodology used here could be replicated elsewhere in New Zealand.

FUTURE WORK

For drying and wetting studies for the Firth, refine the wetting-and-drying projections in further detail by

- Scenario modelling of catchment flows and sediment runoff under different socio-economic policy settings (we had hoped to do that in the case study, but that has proved impractical in the time and resources available)
- Contrasting model results to sedimentation rates estimated from stable isotopes in coring samples, compared to climate records of wind speeds and direction, and river discharges
- Using the Water Column sediment model to adjust morphology of the inner Firth of Thames and run SLR hydrodynamic scenarios

For mangrove distributions

- Clarify the potential impacts of both shallow and deep subsidence, to determine implications of infrastructure and other coastal barriers that may prevent shoreward migration of coastal habitats, and to improve quantification of the impacts of different land-use policies on sediment supply

For hydrological modelling

- Build in landuse change and other socio-economic related factors into the TopNet model
- Assess the sensitivity of the flow projections to the modelled spatiotemporal precipitation variability

For flooding and salinity intrusion studies

- Analyse extreme water levels in the upper Ohinemuri River
- Examine the influence of spring/neap tides and storm surges
- Test the sensitivity of the downstream water level to weighting the joint probability to either of the two rivers
- Investigate the effect of climate change and land-use on extreme river floods for a given ARI.

Economic and land use scenario modelling

- Explicitly account for local population and urban growth dynamics
- Improved integration with biophysical models
- Assess flood and sea level rise impact on land availability and suitability
- Incorporate impacts of carbon sequestration from mangroves

ACKNOWLEDGEMENTS

We acknowledge funding through the Ministry of Business, Innovation and Employment as part of project "Climate change impacts and implications" (contract C01X1225). We acknowledge the World Climate Research Programme's Working Group on Coupled Modelling, which is responsible for CMIP for producing and making available their model output. Helpful discussions have been held with Rick Leifting (Waikato Regional Council), Dr Malcolm Green (Streamlined consultants) and Professor Giovanni Coco (Auckland University).

REFERENCES

Ackerley, D., Bell, R.G., Mullan, A.B., McMillan, H. (2013) Estimation of regional departures from global-average sea-level rise around New Zealand from AOGCM simulations. *Weather & Climate* 33: 2–22. Journal of the Meteorological Society of New Zealand (Inc).

Balke, T., Swales, A., Lovelock, C.E., Herman, P.M.J., Bouma, T.J. (2015) Limits to seaward expansion of mangroves: Translating physical disturbance mechanisms into seedling survival gradients. *Journal of Experimental Marine Biology and Ecology* 467: 16–25. http://dx.doi.org/10.1016/j.jembe.2015.02.015

Bashar, K., Hossain, M. (2006) Impact of sea level rise on salinity of coastal area of Bangladesh. 9th *International River Symposium. Brisbane, Australia*.

Cameron, M. (2013) The demographic implications of climate change for Aotearoa New Zealand: A review. pp Page, NIDEA Working Paper WP-4. Hamilton: National Institute of Demographic and Economic Analysis, University of Waikato.

Church, J.A., White, N.J. (2011) Sea-level rise from the late 19th to the early 21st century. *Surveys in Geophysics* 32: 585–602. doi:10:1007/s10712-011-9119-1.

Church, J.A., P.U. Clark, A. Cazenave, J.M. Gregory, S. Jevrejeva, A. Levermann, M.A. Merrifield, G.A. Milne, R.S. Nerem, P.D. Nunn, A.J. Payne, W.T. Pfeffer, D. Stammer and A.S. Unnikrishnan, (2013) Sea level change. Chapter 13. In: Climate Change 2013: The physical science basis. Contribution of Working Group I to the Fifth Assessment Report of the Intergovernmental Panel on Climate Change [Stocker, T.F., D. Qin, G.-K. Plattner, M. Tignor, S.K. Allen, J. Boschung, A. Nauels, Y. Xia, V. Bex and P.M. Midgley (eds.)]. Cambridge University Press, Cambridge, United Kingdom and New York, NY, USA.

Clark, M. P., Rupp, D. E., Woods, R. A., Zheng, X., Ibbitt, R. P., Slater, A. G., Schmidt, J., and Uddstrom, M. J., (2008). Hydrological data assimilation with the ensemble Kalman filter: Use of streamflow observations to update states in a distributed hydrological model. *Advances in Water Resources*, 31, 1309– 1324, doi:10.1016/j.advwatres.2008.06.005.

Daigneault, A., Greenhalgh, S., Samarasinghe, O. (2014) A response to Doole and Marsh (2013) article: methodological limitations in the evaluation of policies to reduce nitrate leaching from New Zealand agriculture. *Australian Journal of Agricultural and Resource Economics* 58: 281–290.

Duan, Q., S. Sorooshian, and V. Gupta (1992) Effective and efficient global optimization for conceptual rainfall-runoff models, *Water Resources Research*, 28(4), 1015–1031, doi:10.1029/91WR02985.

Dymond, J.R., Betts, H.D., Schierlitz, C. (2010) An erosion model for evaluating land-use scenarios. *Environmental modelling and software* 25: 289–298.

Ebi, K.L., Hallegatte, S., Kram, T., Arnell, N.W., Carter, T.R., Edmonds, J., Kriegler, E., Mathur, R., O'Neill, B.C., Riahi, K., Winkler, H., Vuuren, D.P.V., Zwickel, T., 2013. A new scenario framework for climate change research: background, process, and future directions. *Climatic Change* 122: 363–372.

Fæhn, T., Isaksen, E., Jacobsen, K., Strøm, B. (2013) MSG-TECH: Analysis and documentation of a general equilibrium model with endogenous climate technology adaptations. Report available at: http://www.cree.uio.no/publications/2013_23/RAPPORT_MSG_TECH_CREEWP.pdf

Fernandez, M., Daigneault, A. (2015) The Climate Mitigation, Adaptation and Trade in Dynamic General Equilibrium (CLIMAT-DGE) model. Landcare Research Contract Report LC2156 for the Ministry for the Environment.

Golledge, N.R., Kowalewski, D.E., Naish, T.R., Levy, R.H., Fogwill, C.J., Gasson, E.G.W. (2015) The multi-millennial Antarctic commitment to future sea-level rise. *Nature* 526: 421–425 (2015). doi:10.1038/nature15706.

Green, M., Zeldis, J. (2015) Firth of Thames water quality and ecosystem health - a synthesis. NIWA Client Report, Waikato Regional Council Document #: 3316464: 177 p.

Hannah, J., Bell, R.G. (2012) Regional sea level trends in New Zealand. *Journal of Geophysical Research: Oceans* (1978–2012), 117(C1).

IPCC (2007). Climate Change 2007: Synthesis ReportContribution of Working Groups I, II and III to the Fourth Assessment Report of the Intergovernmental Panel on Climate Change Core Writing Team, Pachauri, R.K. and Reisinger, A. (Eds.) IPCC, Geneva, Switzerland. pp 104.

IPCC, 2014. Climate Change 2014: Synthesis Report. Contribution of Working Groups I, II and III to the Fifth Assessment Report of the Intergovernmental Panel on Climate Change [Core Writing Team, R.K. Pachauri and L.A. Meyer (eds.)]. Geneva, Switzerland. 151 pp.

Kakeh, N., Coco, G., & Marani, M. (2016). On the morphodynamic stability of intertidal environments and the role of vegetation. *Advances in Water Resources* 93: 303–314.

Kettles, H.; Bell, R.G. (2015). Estuarine ecosystems. *In*: Robertson H, Bowie S, White R, Death, R, Collins D (Eds.) 2015: Freshwater Conservation under a Changing Climate - Proceedings of a workshop hosted by the Department of Conservation, 10-11 December 2013, Wellington. DOC publication. Christchurch.

Keller, E.D., Baisden, W.T., Timar, L., Mullan, B., Clark, A. (2014) Grassland production under global change scenarios for New Zealand pastoral agriculture. *Geoscience Model Development* 7: 2359–2391.

Kirschbaum, M.U., Watt, M.S. (2011) Use of a process-based model to describe spatial variation in Pinus radiata productivity in New Zealand. *Forest Ecology and Management* 262(6): 1008–1019.

Kirschbaum, M.U.F., Watt, M.S., Tait, A., Ausseil, A-G.E. (2012) Future wood productivity of Pinus radiata in New Zealand under expected climatic changes. *Global Change Biology* 18: 1342–1356.

Lovelock, C.E., Sorrell, B.K., Hancock, N., Hua, Q., Swales, A. (2010) Mangrove Forest and Soil Development on a Rapidly Accreting Shore in New Zealand. Ecosystems 13(3): 437-451. 10.1007/s10021-010-9329-2

Marani, M.; D'Alpaos, A.; Lanzoni, S.; Carniello, L.; Rinaldo, A. (2010). The importance of being coupled: Stable states and catastrophic shifts in tidal biomorphodynamics. *Journal of Geophysical Research–Earth Surface* 115 F04004.

McMillan, H.K., Hreinsson, E.O., Clark, M.P., Singh, S.K., Zammit, C., and Uddstrom, M.J. (2013) Operational hydrological data assimilation with the recursive ensemble Kalman Filter. *Hydrological Earth System Science*, 17, 21-38.

MfE (2016) Coastal hazards and climate change: Guidance for local government. Draft version, Ministry for the Environment. Publication expected in late November, 2016.

MoH (2008) Drinking-water Standards for New Zealand 2005 (Revised 2008), Ministry of Health: 163.

Morrisey, D.J., Swales, A., Dittmann, S., Morrison, M.A., Lovelock, C.E. and Beard, C.M. (2010) The Ecology and Management of Temperate Mangroves. *Oceanography and Marine Biology: An Annual Review* 48: 43–160.

O'Neill, B.C., Kriegler, E., Riahi, K., Ebi, K.L., Hallegatte, S., Carter, T.R., Mathur, R. and Vuuren, D.P. (2013) A new scenario framework for climate change research: the concept of shared socioeconomic pathways. *Climatic Change* 122: 387–400.

Pritchard, M., Swales, A. and Green, M. (2015) Influence of buoyancy- and wind-coupling on sediment dispersal and deposition in the Firth of Thames, New Zealand. Australasian Coasts & Ports Conference 2015, September.

Swales, A., Bentley, S.J. Snr., Lovelock, C.E. (2015) Mangrove-forest evolution in a sediment-rich estuarine system: opportunists or agents of geomorphic change? *Earth Surface Processes and Landforms* 40: 1672–1687.

Thornton, P.E., Law, B.E., Gholz, H.L., Clark, K.L., Falge, E., Ellsworth, D.S., Goldstein, A.H., Monson, R.K., Hollinger, D., Falk, M., Chen, J. (2002) Modeling and measuring the effects of disturbance history and climate on carbon and water budgets in evergreen needleleaf forests. Agricultural and Forest Meteorology 13(1): 185–222.

Thornton, P.E., Running, S.W., Hunt, E.R. (2005) Biome-BGC: terrestrial ecosystem process model, Version 4.1.1. Model product. Available on-line [http://www.daac. ornl. gov] from Oak Ridge National Laboratory Distributed Active Archive Center, Oak Ridge, Tennessee, USA.

Van Vuuren DP, Edmonds J, Kainuma M, Riahi K, Thomson A, Hibbard K, Rose SK, (2011) The Representative Concentration Pathways: An Overview. *Climatic change* 109: 5–31.

van Vuuren, D.P., Carter, T.R. (2013) Climate and socio-economic scenarios for climate change research and assessment: reconciling the new with the old. *Climatic Change* 122: 415–429.

Werner, A.D., Simmons, C.T. (2009) Impact of Sea-Level Rise on Sea Water Intrusion in Coastal Aquifers. *Ground Water* 47(2): 197-204. 10.1111/j.1745-6584.2008.00535.

Zhang, E., Savenije, H.H.G., Wu, H., Kong, Y., Zhu, J. (2011) Analytical solution for salt intrusion in the Yangtze Estuary, China. *Estuarine, Coastal and Shelf Science* 91(4): 492-501. http://dx.doi.org/10.1016/j.ecss.2010.11.008

APPENDIX

Future CO_2 concentration scenarios

These are shown on Figure 22, in which

- RCP2.6 represents a low-emission mitigation pathway, requiring removal to achieve a decline in atmospheric CO_2 by 2050
- RCP8.5 is the high emission scenario.
- The two middle pathways (RCP4.5 and 6.0) require stabilisation of emissions at different time points during the 21st Century.

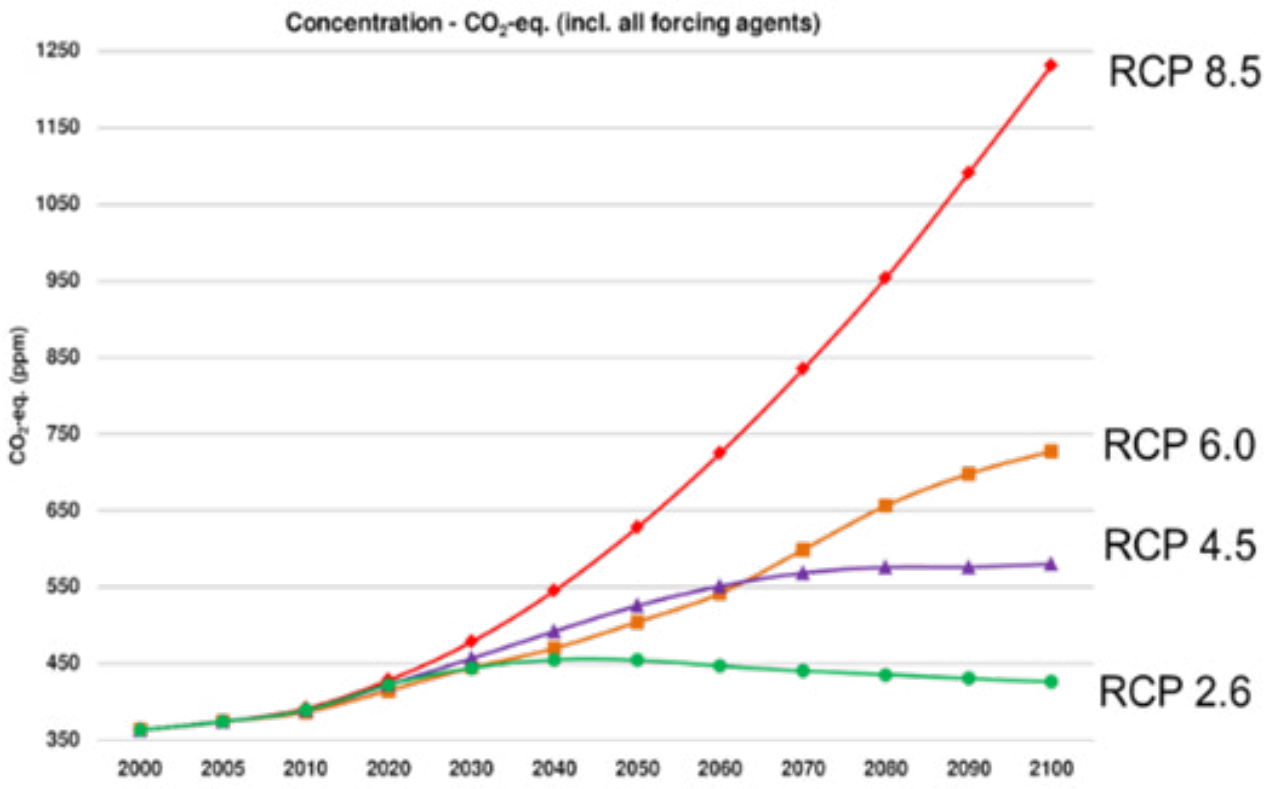

Figure 22 Atmospheric CO_2-equivalent concentrations (in parts-per-million-by-volume) under the four Relative Concentration Pathways (RCPs) (van Vuuren et al., 2011).

Computational Grid

The dense computational grid used for modelling circulation patterns and river salinity is shown on Figure 23.

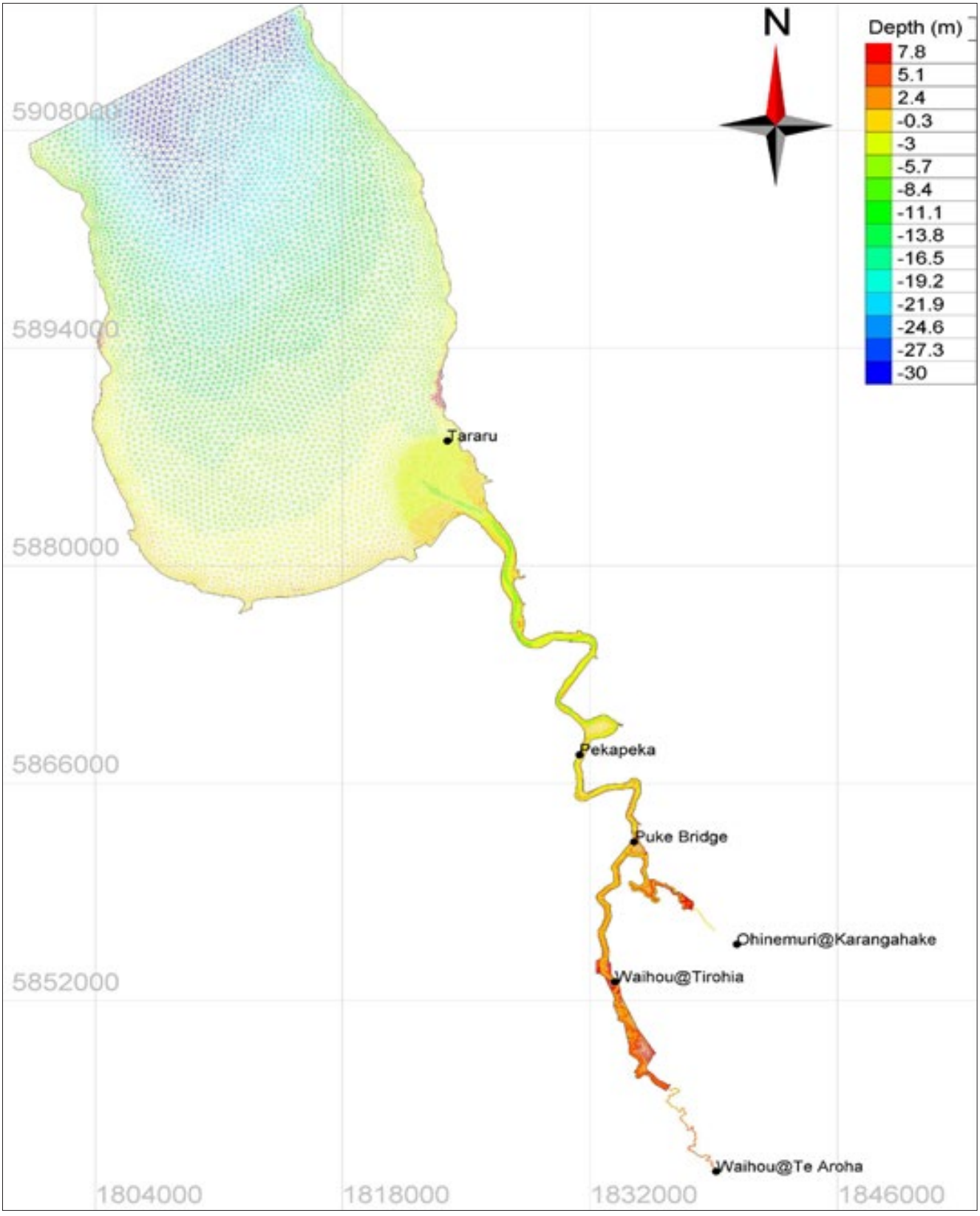

Figure 23 Computational grid.

Derivation of simplified tidal sedimentation model and its numerical solutions

Following the lead of Marani et al. (2010) we consider tidal variations of sediment dynamics in a water column centred on some point in a shallow tidal platform in the horizontal plane. Over a tidal cycle there is loss of sediment from that column in the vertical direction to the bed via settling, but also import or export of sediment from surrounding waters and sediments. At the same time, under SLR (sea level rise), the mean water level is gradually increasing. We call this a "Water Column Model" (WCM)[7]. It is aimed at indicating whether water depth at various points in the Firth will increase or decrease with time, i.e., whether the rate of SLR exceeds the rate of sediment accumulation on various Firth tidal platforms.

We simplify matters further by specifying a constant tidal amplitude and period (ignoring the spring-neap cycle).

No drying and wetting

Consider a shallow-water tidal platform, as shown by the dark blue water region in Figure 24. This platform abuts a deeper open-water channel which exchanges sediment with the water above the platform. It is subject to gains in height (above an arbitrary datum) via sediment deposition and trapping, but also to loss of height via erosion. To predict changes in the water depth above a tidal platform over time we derive a mass balance equation for the change in bed elevation and then another for sediment concentration (C) in the water overlying a tidal flat, with specified (constant) concentration (C_0) in the open water.

Associated tidal variables are defined on Figure 24.

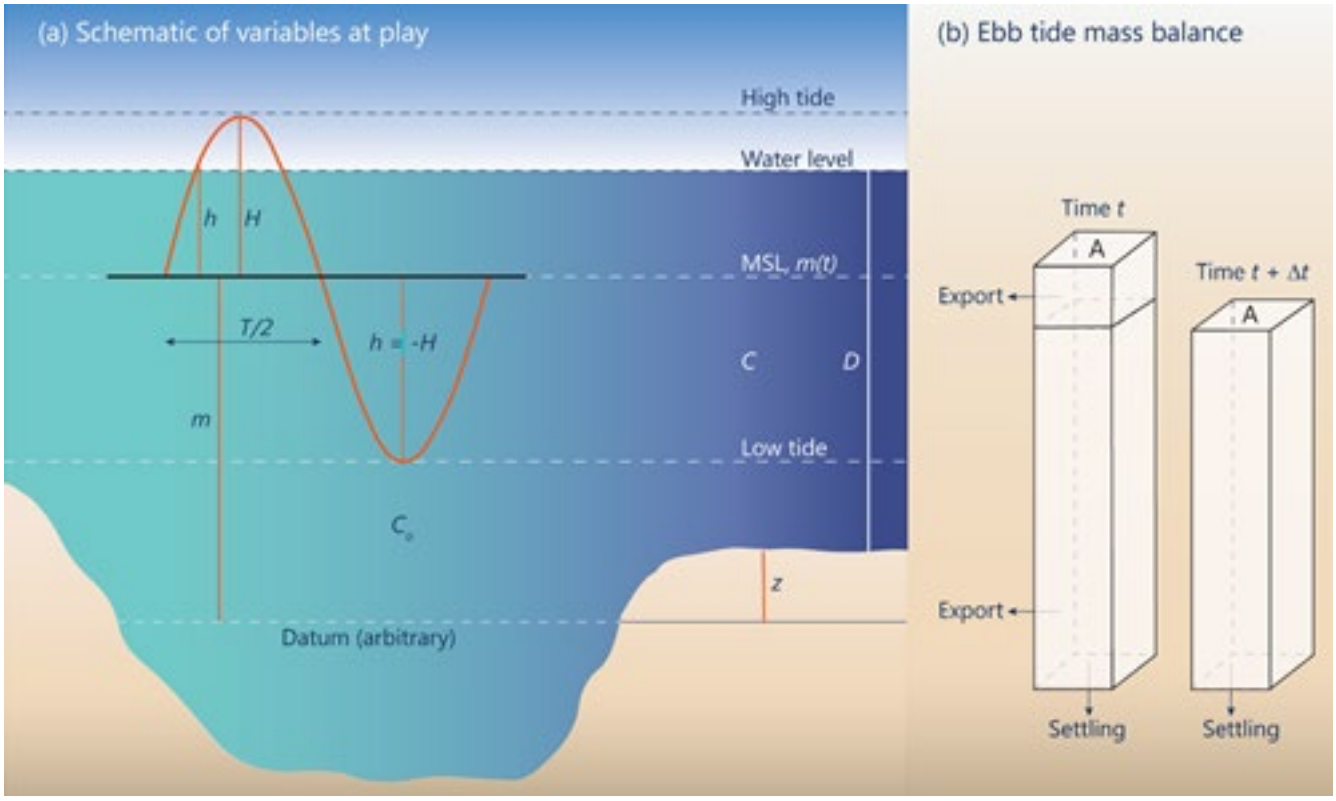

Figure 24 Definition of terms.

The bed elevation mass balance requires that

$$\frac{dz}{dt} = Q_s(z,B) + Q_T(z,B) - E \qquad (1)$$

[7]At first we described this as a "0D" or "point" model, because it lacks explicit horizontal coordinates and is referenced to a point in that plane. However that doesn't capture the vertical and horizontal processes actually incorporated (settling, trapping and erosion). But it isn't a "1D" model either, because it lacks a series of vertical nodes down the water column, as is implied by that term. WCM (Water Column Model) therefore seems the most appropriate descriptor.

where z (units: L) is tidal platform elevation above an arbitrary datum (see Figure 24), t is time, Q_S, Q_T, and E are specific setting, trapping and erosion rates (units: L/T), and B is the "aboveground halophytic vegetation biomass density" (units: M/L^3).[8]

Writing eqs 2 & 3 of Marani et al. (2010) in instantaneous form we have the settling rate

$$Q_S(z,B,t)=\frac{w_s}{\rho_b}C(z,B,t) \tag{2}$$

where w_s is settling velocity (L/T), ρ_b is sediment bulk density (units: M/L^3), C is water-column sediment concentration (units: M/L^3). The trapping rate is given by

$$Q_T(z,B,t)=\frac{\alpha B^{\beta}}{\rho_b}C(z,B,t) \tag{3}$$

where ß is a dimensionless power exponent and α is a scale factor [units: (L/T)(L^2/M)^{ß}]. Therefore, combining eqs (1) – (3),

$$\frac{dz}{dt}=\phi C-E:\quad \phi=\frac{w_s+\alpha B^{\beta}}{\rho_b} \tag{4}$$

where φ is a constant [units: L^4/(MT)].

The concentration equation required by eq (4) (also eq. 4 in Marani *et al*. 2010) is

$$\begin{aligned}\frac{d(DC)}{dt}&=-w_sC-\alpha B^{\beta}C+\tilde{C}\frac{dh}{dt}\\&=-\phi\rho_bC+\tilde{C}\frac{dh}{dt}\end{aligned} \tag{5}$$

with $C_{t=0}=C_0$ and where $D(t)$ is the instantaneous water depth (L), $m(t)$ is the mean sea level referenced to the same datum used for z, $h(t)$ is the instantaneous water surface elevation above or below mean sea level (L) and $\tilde{C}$ (units: M/L^3) is given by

$$\tilde{C}(z,B,t)=\begin{cases}C(z,B,t) & \text{when}\quad \frac{dh}{dt}\le 0\quad \text{(ebb)}\\ C_0 & \text{when}\quad \frac{dh}{dt}\ge 0\quad \text{(flood)}\end{cases} \tag{6}$$

The depth D is independent of the datum and is given by

$$D(t)=m(t)+h(t)-z(t) \tag{7}$$

The tidal amplitude at time t [$h(t)$] is

$$h(t)=H\cos\left(\frac{2\pi t}{T}\right):h(0)=H \tag{8}$$

[8]See units on Y-axis of Figure 4 of Marani et al. (2010). As is common in ecological modelling a "density" refers to mass mas per unit area whereas "bulk density" is mass per unit volume.

where H is the tide's half-amplitude (L) and T is the tidal period [so that at $h(0) = H$ at high tide and $h(T/2) = -H$ at low tide]. H and T are assumed constant.

Ebb tide numerical solutions

During each tidal cycle we hold m and z constant (= M and Z), and update them at the end of each tidal cycle. Note that for there to be a positive water depth at low tide (no drying and wetting), we require that

$$D_{\min} > 0 \quad \text{and so} \quad M > H + Z \tag{9}$$

To be assured that the model properly conserves mass, it is wise to re-derive its equations from first principles. So, assuming complete instantaneous mixing over the water depth, the sediment mass balance over a period Δt is

$$\underbrace{(DAC)^{t+\Delta t} - (DAC)^{t}}_{\text{Change in storage}} = \underbrace{-\xi\left(\overline{AC}\right)\Delta t}_{\text{Settling}} + \underbrace{\left(\overline{AC\frac{dh}{dt}}\right)\Delta t}_{\text{Net Export}} \tag{10}$$

where ξ is the effective sediment settling velocity [L T^{-1}, see eq. (12)] and the overbars represent time-averages. Cancelling out the constant area (A), dividing throughout by Δt, and going to the limit ($\Delta t \rightarrow 0$), we obtain

$$\frac{d(DC)}{dt} = -\xi C + C\frac{dh}{dt} \tag{11}$$

Note that for a flood tide (see section 10.3.3) the last term would include C_0 rather than C (C_0 is the concentration of sediment in the deeper "lagoon" water, shown in Figure 24): this is consistent with eq. (6).

Referring to eq. (5) we have

$$\xi = \phi\rho_b = w_s + \alpha B^{\beta} \tag{12}$$

We approximate (11) using simple differencing of time-derivatives, cancelling throughout by the plan-cross-section-area (A) and time-weighting of the concentrations on the right-hand-side as

$$\frac{\left(h^n + M - Z\right)C^n - \left(h^{n-1} + M - Z\right)C^{n-1}}{\Delta t} = -\xi\left(wC^n + \overline{w}C^{n-1}\right) + \left(wC^n + \overline{w}C^{n-1}\right)\left(\frac{h^n - h^{n-1}}{\Delta t}\right) \tag{13}$$

where Δt is the time step such that $\Delta t = t^n - t^{n-1}$ and $\overline{w} = 1 - w$: $0 \leqslant w \leqslant 1$.

We can restate eq. (13) with the unknown C^n on the left-hand-side and all the knowns on the right, i.e.,

$$C^n = \left[\frac{D^{n-1} - \overline{w}\xi\Delta t + \overline{w}\left(h^n - h^{n-1}\right)}{D^n + w\xi\Delta t - w\left(h^n - h^{n-1}\right)}\right] C^{n-1} \tag{14}$$

where D^n (= $h^n + M - Z$) is the water depth at time $t = n\Delta t$.

Flood tide numerical solutions

Here the mass balanced equation (11) becomes

$$\frac{\mathrm{d}(DC)}{\mathrm{d}t} = -\xi C + C_0 \frac{\mathrm{d}h}{\mathrm{d}t} \tag{15}$$

which we discretise as

$$\frac{\left(h^n + M - Z\right)C^n - \left(h^{n-1} + M - Z\right)C^{n-1}}{\Delta t} = -\xi\left(wC^n + \overline{w}C^{n-1}\right) + C_0\left(\frac{h^n - h^{n-1}}{\Delta t}\right) \tag{16}$$

again, collecting terms, we get a direct equation for C^n, i.e.,

$$C^n = \left(\frac{D^{n-1} - \overline{w}\xi\Delta t}{D^n + w\xi\Delta t}\right) C^{n-1} + \left(\frac{h^n - h^{n-1}}{D^n + w\xi\Delta t}\right) C_0 \tag{17}$$

Drying and wetting

Special cases arise when the tidal platform becomes exposed and is re-covered during a time step, as depicted on Figure 25.

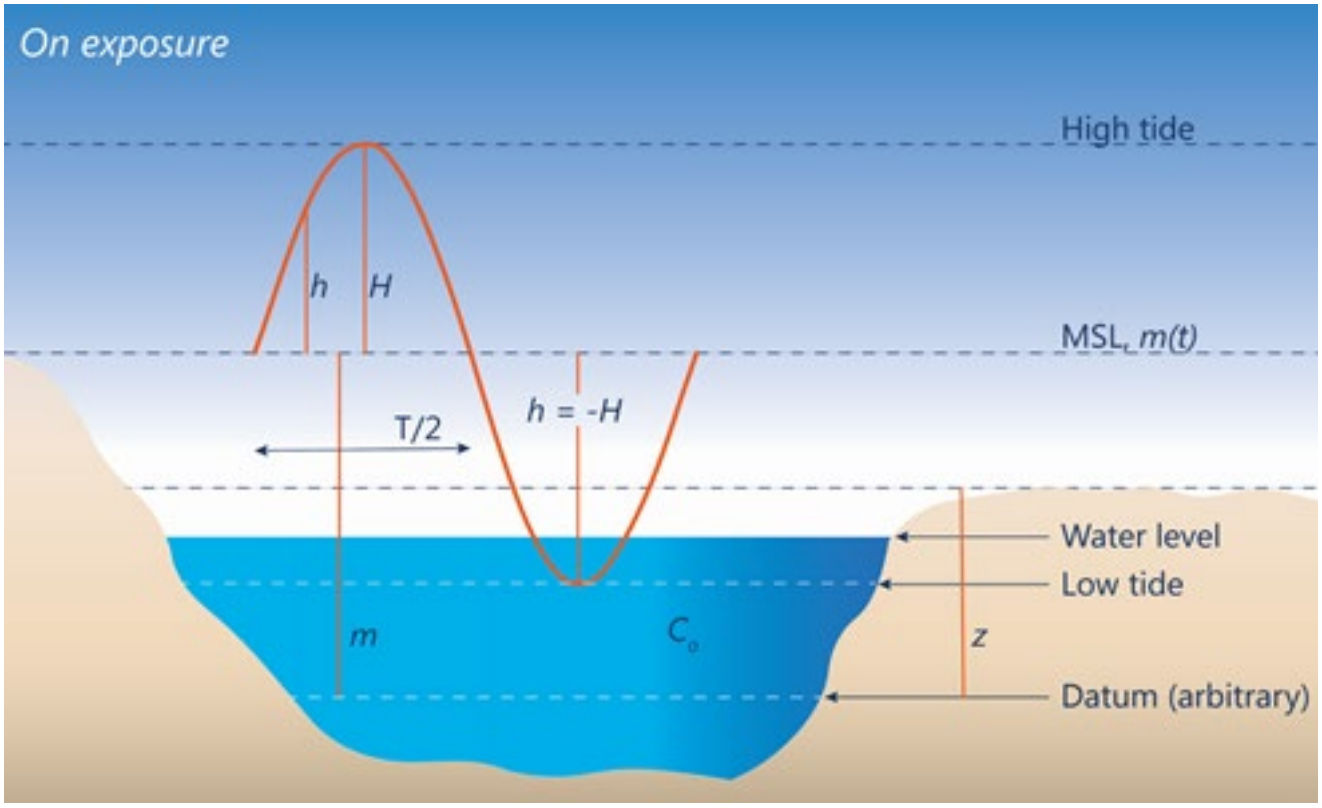

Figure 25 Exposure toward low tide (when m + h ≤ z), i.e., drying and wetting.

Time of first exposure

Denote by t^* the time at which exposure first occurs, i.e., when $t^{n-1} < t^* < t^n$ and so $\Delta t^* = t^* - t^{n-1} < \Delta t$, it being understood that these n and * values refer to the ebb tide exposure event. We cannot calculate a concentration at t^* because $C(t^*)$ is undefined. We could try to calculate a value for $C(pt^*)$, where the proportion p is a tiny bit less than 1. However the mass contained in the very shallow water in the time interval Δt^* is negligible, so it seems best to not attempt this (if it is of concern then reduce the time step).

Note that the time of exposure is simply obtained from

$$t^*_{\text{exposure}} = \left(\frac{T}{2\pi}\right)\cos^{-1}\left(\frac{Z-M}{H}\right) \tag{18}$$

Time of re-covering

Now denote by t^* the time at which re-covering occurs, i.e., $t^n-1 < t^* < t^n$ and so $\Delta t^* = t^n - t^*$, it being understood that these n and * values now refer to the flood tide re-covering event. Then, noting that C^{n-1} is no longer defined and (again) that the time-interval has been shortened, we must modify (17) to become

$$C^n = \lambda_{\text{recovery}}\, C_0 : \quad \lambda_{\text{recovery}} = \frac{h^n - h^*}{D^n + \xi \Delta t^*} \tag{19}$$

Note that the time-weighting coefficient (w) has been set to 1 in this equation—because C^{n-1} is undefined we can only take a fully implicit approach for this time interval.

The value of t^* for time of recovery is simply obtained from

$$t^*_{\text{recovery}} = T - t^*_{\text{exposure}} \tag{20}$$

Without these emendations some very untidy "blips" arise around exposure and recovery events.

Updating the depth

Note that Z and M are kept constant within each tidal cycle. M can be updated at the end of each tidal cycle (under SLR it will have a tiny increment) and Z can be updated with the procedures of Marani et al. (2010) (which they updated annually, but we update after each tidal cycle).

Erosion (E) in the model is expressed as a function of bed shear stress (τ) generated by tidal currents (τ_c) and wind waves (τ_w), and the critical bed shear stress of erosion (τ_{cr}). τ_{cr} depends of the size fraction of the sediment grains. When $\tau > \tau_{cr}$ sediment is eroded on the platform and when $\tau < \tau_{cr}$, sediment can deposit thereon. The erosional effects of the tide are mainly effective in deeper water. Therefore, in the shallow waters under consideration, the effects of wind waves are assumed the main source of erosion and mobilisation of sediments.

τ_w in the model is computed from wind speed, fetch length, and water depth from standard formulas described in Kakeh et al. (2016). The wind speeds for our simulations were sourced for a central location in the Firth of Thames from each climate model and each RCP scenario.

Changes in water depths predicted using six down-scaled GCM models

Here we present the high-tide water depths predicted by the Water Column Model for six down-scaled Global Circulation Models. All cases consider a drying and wetting intertidal platform with initial high-tide water depths (D) of (a) D = 0.7 m; (b) D = 1.5; (c) D = 2.0 m, all with tidal range = 1 m, based on four RCPs, leading to changes in wind and sea level rise. In all cases the model has a constant sediment delivery manifest as open water concentration of 300 g m^{-3} (i.e., in Figure 24 and Figure 25, C_0 = 300 g m^{-3}). Results for percentage changes in sediment delivery are not shown (but see Figures 8 – 10 for projections related to changes in sediment delivery for the Hadley model).

HadGEM2-ES MOHC (UK)

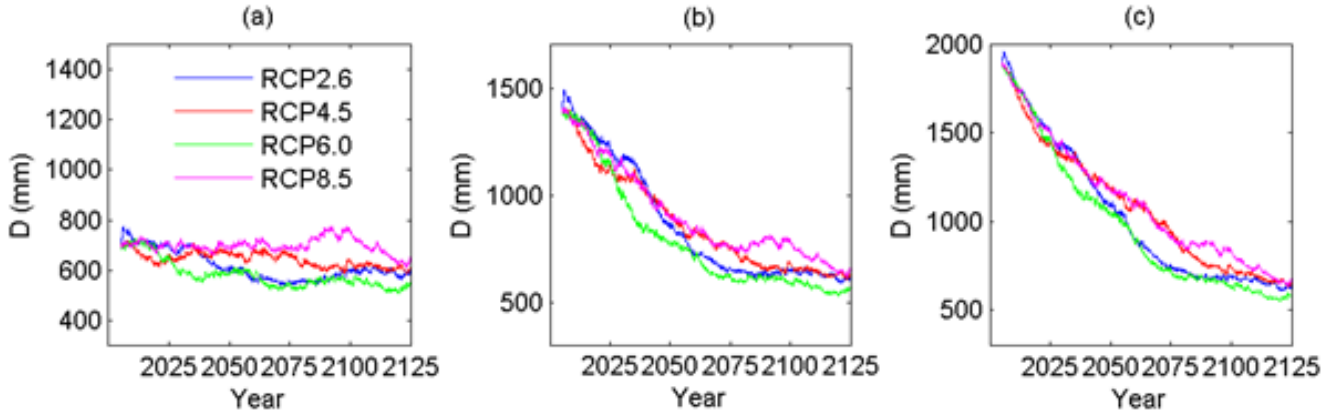

CESM1-CAM5 NSF-DOE-NCAR (USA)

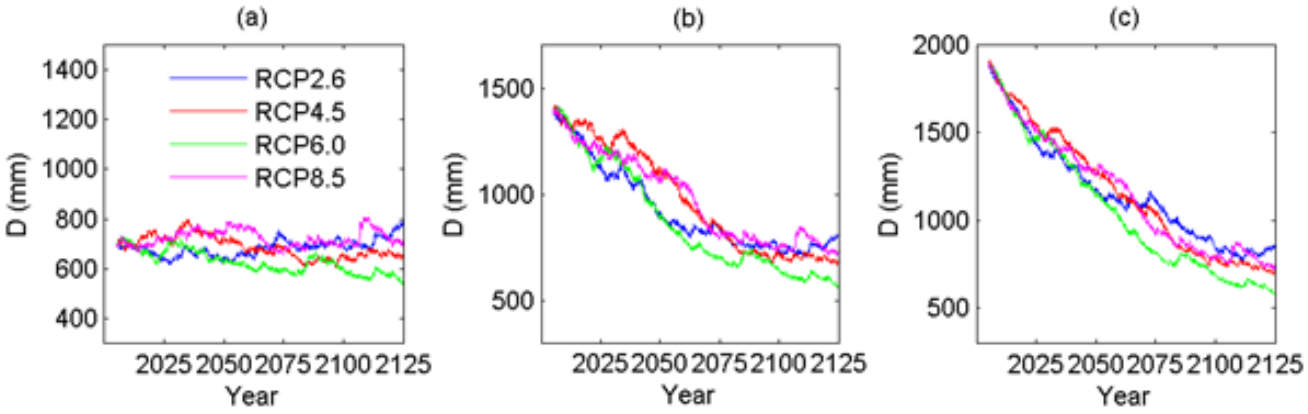

NorESM1-M NCC (Norway)

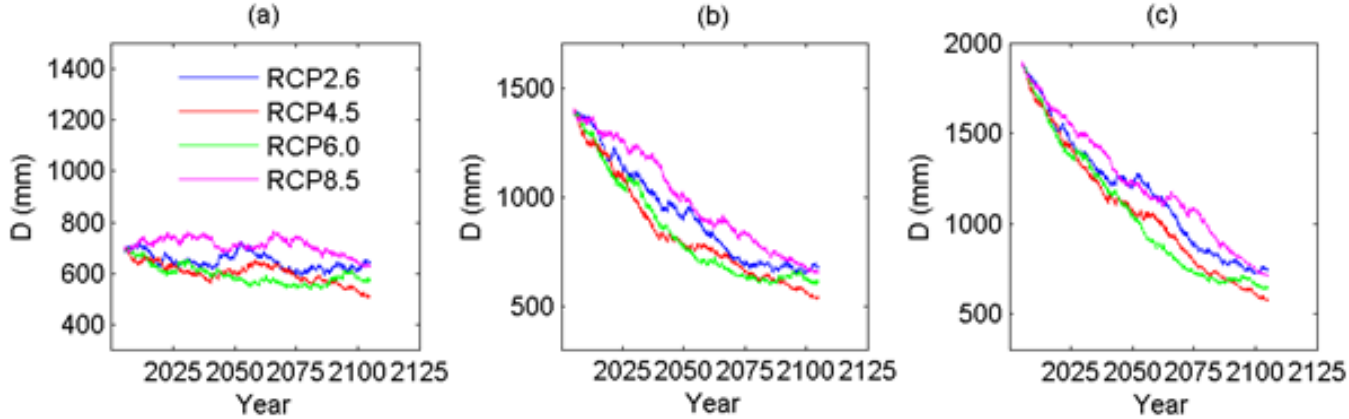

GFDL-CM3 NOAA-GFDL (USA)

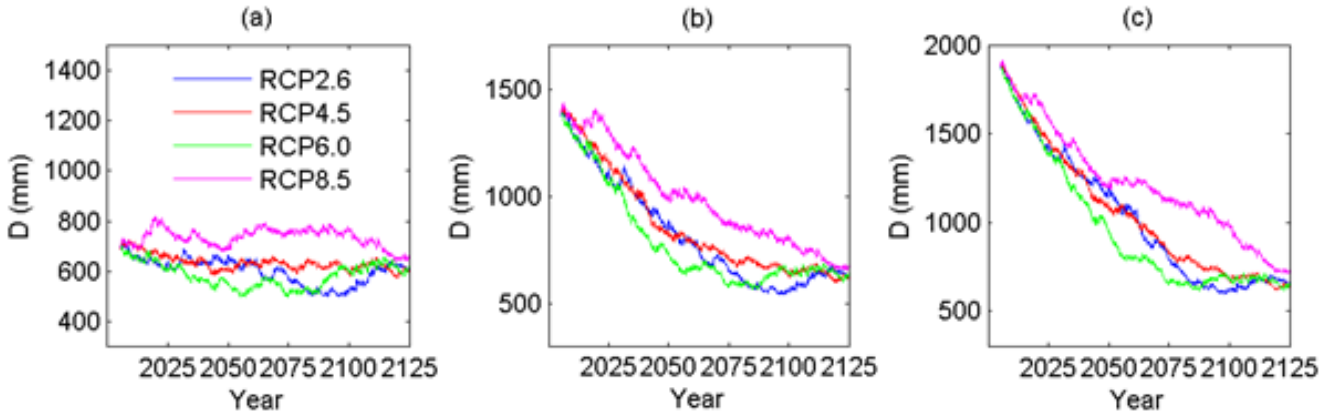

GISS-E2-R NASA-GISS (USA)

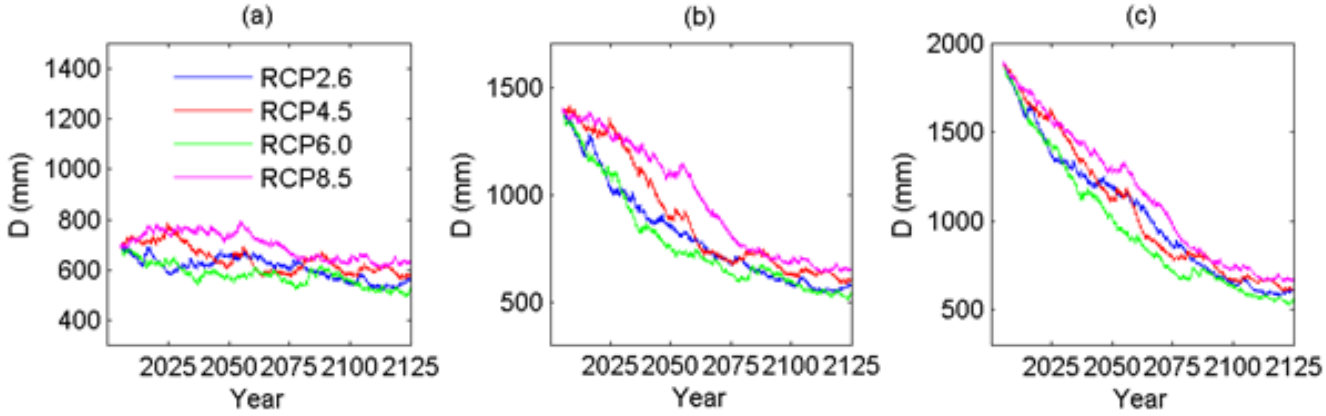

BCC-CSM1.1 BCC (China)

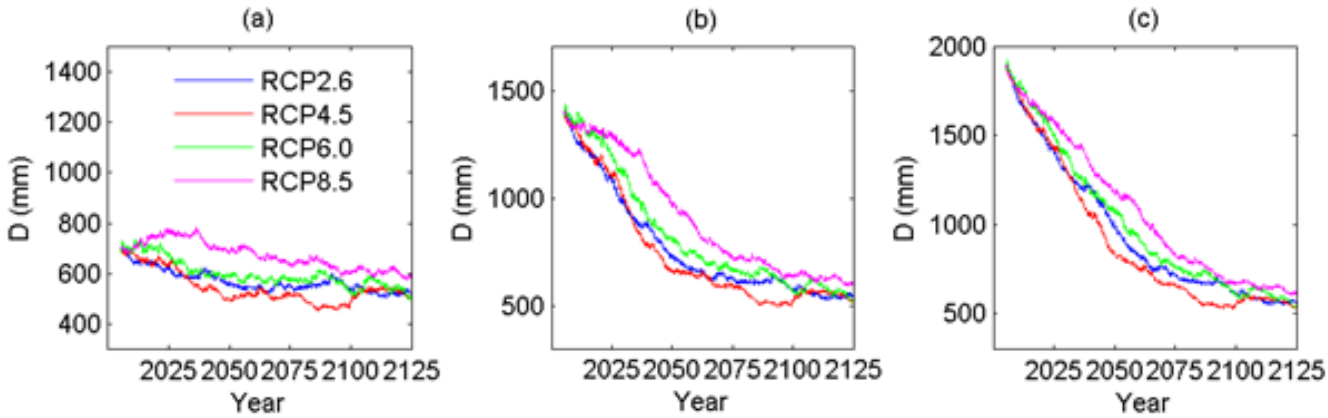

TopNet calibration

Observed streamflow

Review of the measured streamflow indicates that suitable discharge measurements were available at nine locations. In order to limit the potential impact of water consented activities on the calibration of the hydrological model, only seven gauging stations were considered as calibration check sites (Table 6).

TopNet hydrological models were built for the seven surface water catchments (Table 6) based on Strahler 1 catchments (typical size 0.7 km^2). The total number of TopNet catchments in the Hauraki Gulf surface water catchment is 9352 Strahler 1 catchments.

Table 6 Physiographic information for the seven calibrated watersheds

Watershed	Site	Site ID	REC id	Area (km²)	Period of record
Waiomu	Waiomu at Days	9610	3003159	9.6	1985-1991
Tapu	Tapu at Tapu-coroglen Rd	9701	3002756	26.3	1991-2011
Wairoa	Wairoa at Tourist Rd Br	8516	2007413	149.9	1979-2011
Ohinemuri	Ohinemuri at Karangahake	9213	3010506	284.7	1956-present
Waihou	Waihou at Te Aroha Br	9205	3013014	1100.0	1965-present
Piako	Piako at Paeroa Tahuna Rd	9140	3012314	536.7	1972-present
Waitoa	Waitoa at Paeroa Tahuna Rd	9117	3011973	485.4	1972-1983

Calibration methodology

TopNet calibration requires the calibration of parameter multipliers, as one of the main assumptions of TopNet is that the spatial distribution of the parameters is a-priori determined from catchment physiographic information from the sources presented above. TopNet requires the calibration of eight parameter multipliers for each sub-catchment, whose initial values are set to a value of 1. Then the optimization is carried out using the Shuffle Complex Evolution-UA (SCE-UA) method (Duan et al, 1992), which is widely used in hydrologic modelling. Table 7 presents the typical range of the parameter multipliers used during the calibration process.

Table 7 Range of TopNet parameter multipliers used during calibration process

Parameter name (internal name)	Parameter description	Calibrated range
Saturated store sensitivity (topmodf)	Describes exponential decrease of soil hydraulic conductivity with depth	[0.01-2] * default
Drainable soil water (swater1)	Range between saturation and field capacity	[0.05-10] * default
Plant available soil water (swater2)	Range between field capacity and wilting point	[0.05-10] * default
Hydraulic Conductivity at saturation (hydcond0)		[0.1-10000] * default
Overland flow velocity (overvel)		[0.1-10] * default
Manning n	Characterises the roughness of each reach	[0.1-10] * default
Soil water content (dthetat)	soil water content	[0.1-10] * default
Gauge Undercatch (gucatch)	Adjustment for non-representative precipitation	[0.5-1.5] * default

The accuracy of the calibration/validation process is estimated using the following hydrological criteria and statistics:

- Nash-Sutcliffe efficiency coefficient calculated on the discharge (NS) and on the logarithm of the discharge (NS Log). The NS score represents a measure of the residual variance versus the data variance. A NS score of 1 indicates that the calibration perfectly mimics the observations in time and volume. A negative NS score indicates that the average of the observation is a better predictor than the model flow. The NS score represents the ability of the model to mimic the observations during high flow periods, while the NS Log score represents the ability of the model to mimic the observations during low flow periods. Based on the objective of the model, the main objective function was chosen to be the NS score;
- Total water balance of the upstream catchment;
- Comparison of observed and predicted flow duration curves (to identify potential mismatches in the statistical distribution of the flows) and cumulative flow (to identify potential issues related to systematic bias in the calibration process);
- Comparison of observed and predicted average monthly flows over the period of simulation (to identify potential issues on the seasonality of the water balance);
- Comparison of observed and predicted flow deciles over the period of simulation (to identify potential skewness of the calibrated model towards specific flow conditions). The flow decile presented hereafter is subject to some artificial bias towards the low flow values as missing observations were given a value of 0.

As a common calibration period could not be found for all the streamflow gauges, the calibration period was carried out on independent time slices for each catchment aiming to represent diverse hydrological conditions (e.g. annual flow below and above the observed mean annual flow at each of the gauging stations) while validation was carried out over the remaining of the period available at each station. In addition, further care was taken to ensure that the model parameters remained between physically reasonable limits.

Calibration results

For sake of clarity, calibration and validation results are presented only for the Waihou and Piako catchments. Figure 26 presents the daily and observed hydrographs for the Paiko catchment (Paiko at Paeroa Tahuna Rd) over the period 2003-2004, while Figure 27 shows the observed and simulated hydrograph for the Waihou at Te Aroha over the period 2001-2003. Analysis of the simulations indicates that the calibrated models correctly reproduce the hydrological characteristics encountered during the calibration/ validation period during high flow period.

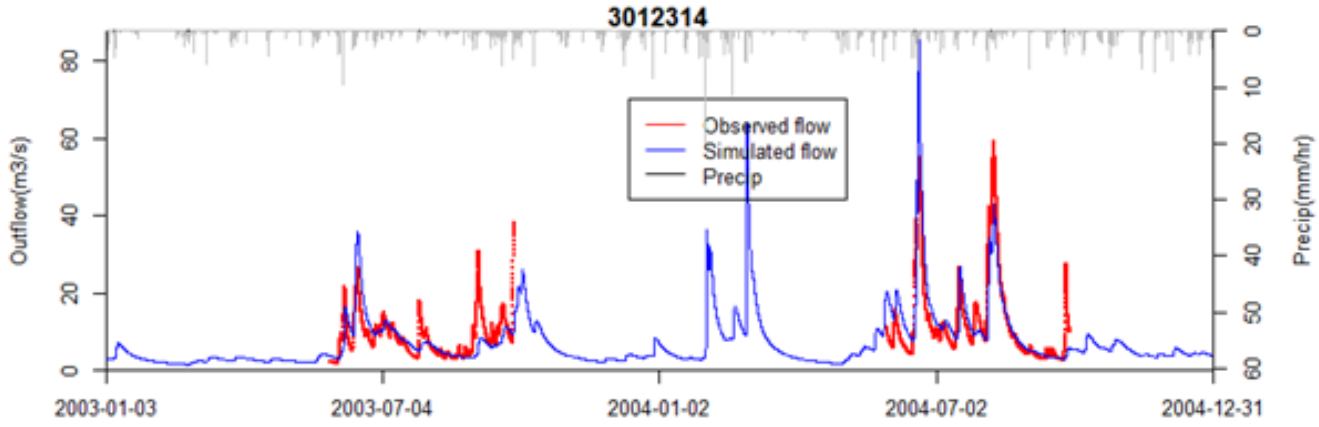

Figure 26 Validation of observed and simulated hydrograph for the Piako at Paeroa Tahuna Rd over 2003–2004. Observed discharged are represented only during winter season to limit impact of water consenting activities on observed discharge during summer season for the Paiko catchment.

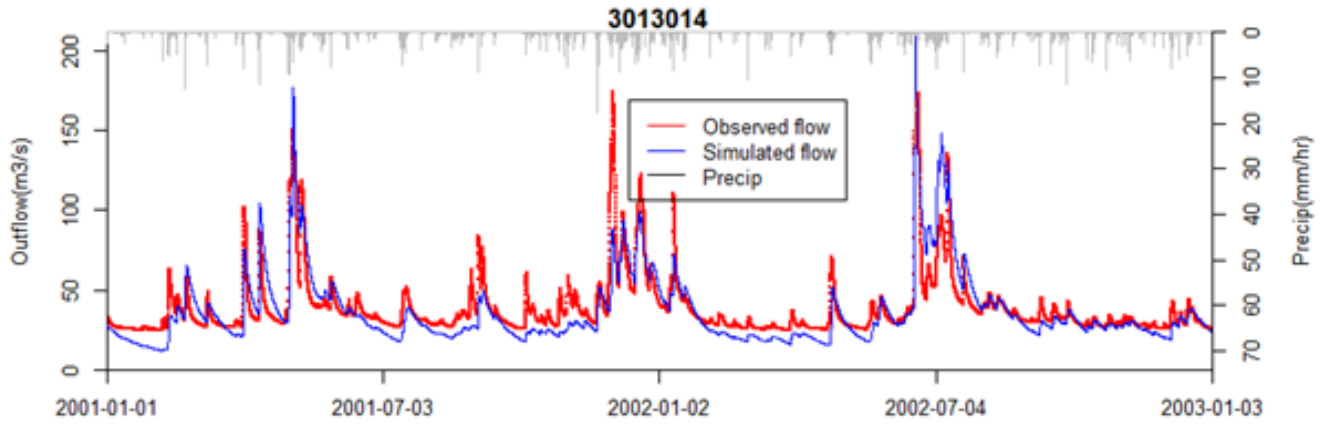

Figure 27 Validation of observed and simulated hydrograph for the Waihou at Te Aroha over 2001-2003.

Changes in saline intrusion predicted using six down-scaled GCM models

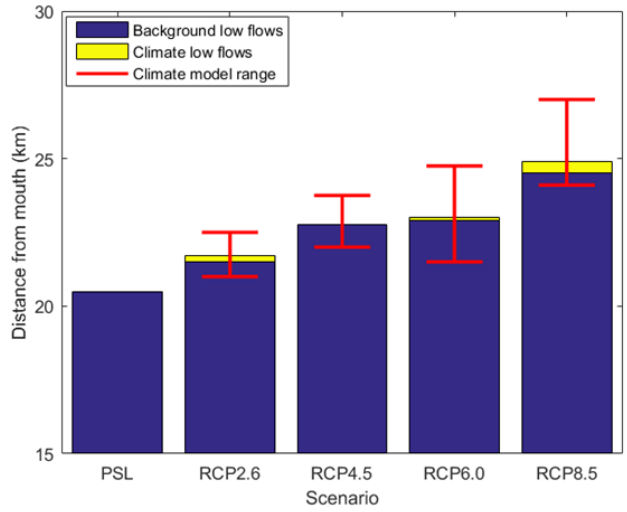

Figure 28 Changes in saline intrusion length predicted for present sea level ("PSL") and for the four RCP values and their predicted mean annual low flows 100 years hence, averaged over the six GCMs. The yellow bands represent the changes attributable to using RCP-related mean annual low flows versus predictions made assuming present-day low flows (regardless of the RCP value). Red bars denote the range of values predicted under the six GCMs.

Scenario models details

Demographic model

We developed a bottom-up sub-national population projections model, wherein gross migration between pairs of regions in New Zealand (n=16) is modelled using a set of age-sex-specific gravity models. Our model allows all inter-regional migration flows to be estimated and projected in a common framework with a single set of assumptions. This method offers a number of advantages over traditional methods, in particular that factors known to affect migration flows (such as climate, etc.) can be explicitly (based on regression modelling) incorporated into the population projections in a transparent and justifiable manner.

The estimated internal migration gravity model demonstrated that climate variables (sunshine, rainfall) had statistically significant but very small effects on internal migration in New Zealand. As such, most of the projected population change in New Zealand is likely to be driven by other factors (e.g. economic factors, population ageing and momentum, etc.), as discussed in Cameron (2013).

Primary production models

Pasture growth modelling

To model pasture growth, we used the Biome-BGC model v4.2 (Thornton et al., 2002, 2005), adapted to two types of New Zealand managed grassland systems: sheep/beef (low intensity) and dairy (high intensity). The Biome-BGC model is an ecosystem process model that simulates the biological and physical processes controlling fluxes of carbon, nitrogen and water in vegetation and soil in terrestrial ecosystems. This includes the CO_2 fertilization effect, which enhances the rate of photosynthesis and reduces water loss in plants under elevated CO_2 atmospheric concentrations. We used the model's built-in C3 grasslands mode, with some key ecological parameters modified and re-interpreted to represent managed pasture and the presence of grazing animals (Keller et al., 2014). Model parameters were calibrated against New Zealand pasture growth data and validated for both dairy and sheep systems as described in Keller et al., 2014. The primary model inputs, daily minimum and maximum temperature, precipitation, vapour pressure deficit, and solar radiation, were derived from the outputs of the 6 GCMs.

Unique parameterizations were assigned to both sheep and dairy 'ecosystems'. The main difference between the two is the intensity of farming: dairy

systems receive more nitrogen inputs (to simulate more fertiliser use), more grass is eaten (in the form of increased whole-plant mortality), and more animal products (milk or meat) are extracted from the system. In addition, the dairy parameterization effectively results in increased water-use efficiency. Note that irrigation is not simulated in either system.

The model was run for each 5 x 5 km VCSN grid square in the Waihou catchment with location-specific weather inputs, soil texture and rooting depth. A reference or 'baseline' pasture production for each GCM was simulated using the RCP past climate input (representative of modern day conditions) and averaged over the nominal years 1985 - 2005. For all future scenarios, the model was first spun up using RCP past climate, and then restarted and run as a transient simulation from 2005 to 2100 using each model- and scenario-specific projected climate.

Forestry

The simulation results described here used the comprehensive process-based ecophysiological model CenW 4.1 to simulate the growth of *Pinus radiata* in the Bay of Plenty region. The model had previously been parameterised for the growth of these trees based on data from the whole of New Zealand (Kirschbaum and Watt, 2011). It had also previously been used for climate-change impact assessments for New Zealand (Kirschbaum et al., 2012), and essentially the same modelling procedure was followed here. It essentially models tree growth over 30 years, with initial stand densities and thinning regimes as described by Kirschbaum et al. (2012).

The novel aspect of the present work is the availability of actual daily output of key weather parameters from six different GCMs for each day up to 2100. In past work, only average changes in weather parameters were available, and theses weather anomalies had to be added to a current-day weather sequence. That preserved a realistic pattern of seasonal changes in weather parameter, but did not include any possible changes in those patterns themselves. The climatic data used here are the direct output from GCM runs and thus include any possible changes in weather patterns (such as changing inter-annual frequency of drought periods, or changes in seasonal temperature or rainfall patterns).

Data are presented both as changes from current (1980-2010) productivity to productivity in 2055 (2040-2070) or 2085 (2070-2100), and as progressive changes by running the model to simulate productivity from 1980-2010, followed by a run with data from 1981-2011 and so on. Further details are given in the following sections.

Economics and land use models

Climat-DGE

To estimate the effect of global SSP on the New Zealand economy, we used the climate and trade dynamic general equilibrium (CliMAT-DGE) model developed by Landcare Research. CliMAT-DGE is a multiregional, multi-sectoral, forward-looking dynamic general equilibrium model with a relatively long time horizon of 100 years or more. This model is suited to studying the efficient (re)allocation of resources within the economy and the response over time to resource or productivity shocks. CliMAT-DGE primarily uses the Global Trade Analysis Project (GTAP) version 8 data set. The base year of the benchmark projection is 2007. The model then develops a benchmark projection of the economic variables and GHG emissions, and simulates scenarios to evaluate the impacts of mitigation policies. Based on long-run conditions and constraints on physical resources, which restrict the opportunity set of agents, the model predicts the behaviour of the economy, energy use, and emissions by region and sector (Fæhn et al. 2013).

CliMAT-DGE covers 18 aggregated production sectors; we focused on the cattle and food sectors. Model dynamics follow a forward-looking behaviour where decisions made today about production, consumption and investment are based on future expectations, estimated in 5-year time steps. The economic agents have perfect foresight and know exactly what will happen in all future periods of the time horizon. Thus, households are able to smooth their consumption over time in anticipation of large price shocks that may arise as a result of resource constraints or environmental taxes. For a thorough description of CliMAT-DGE, see Fernandez & Daigneault (2015).

NZFARM

The New Zealand Forest and Agriculture Regional Model (NZFARM) is a comparative-static, non-linear, partial equilibrium mathematical programming model of New Zealand land use operating at the catchment scale developed by Landcare Research (Daigneault et al. 2012, 2016). In this study it was used to assess how changes in climate (i.e. yields), socio-economic conditions (e.g., commodity prices and

input costs), resource constraints, and environmental policy (e.g., GHG reduction pathways) could affect a host of economic or environmental performance indicators that are important to decision-makers and rural landowners. The version of the model used for this analysis can track changes in land use, land management, agricultural production, freshwater contaminant loads and GHG emissions.

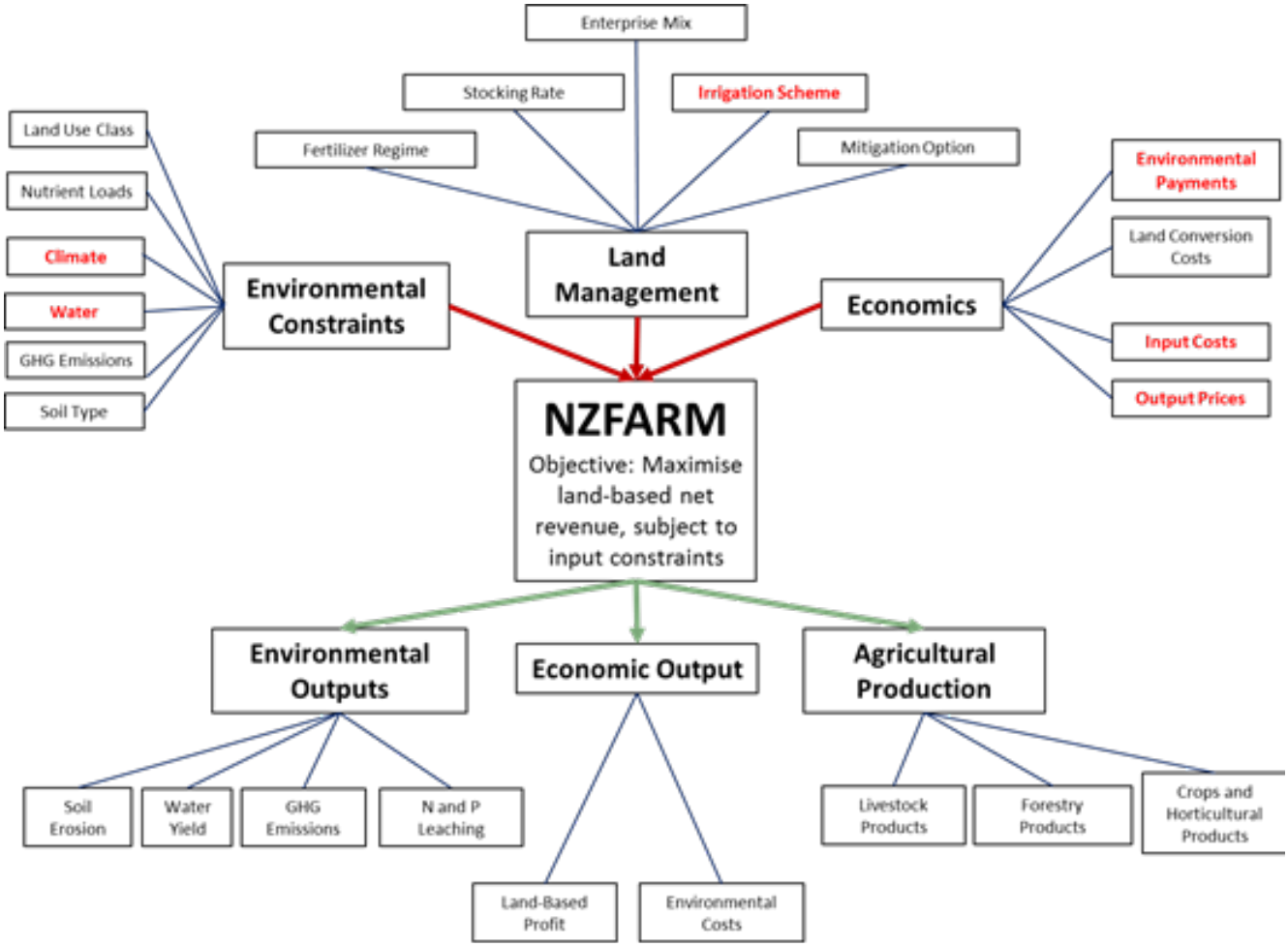

Figure 29. Diagram of inputs and outputs from NZFARM

In this case study, we use NZFARM to assess the implications on farm income, land use and the environment when farmers in the Waihou catchment are faced with variations in agricultural yields due to climate change and/or alternative shared socio-economic pathways. This analysis builds on previous work on climate change impacts on agriculture and forestry in New Zealand by not only indicating the likely impact of climate change on production, but also the effect that landowner adaptation may have on land use, economics, production, and environmental outputs within a simultaneous modelling framework.

The model's objective function maximizes the net revenue of agricultural production, subject to land use and land management options, production costs and output prices, and environmental factors such as soil type, water available for irrigation, and any regulated environmental outputs (e.g. GHG emissions taxes) imposed on the catchment. Catchments can be disaggregated into sub-regions (i.e. zones) based on different criteria (e.g. land use capability, irrigation schemes) such that all land in the same zone will yield similar levels of productivity for a given enterprise and land management option. In this case, each VCSN grid cell is modelled as an individual zone within the Waihou catchment.

Simulating endogenous land management is an integral part of the model, which can differentiate between 'baseline' land use and farm practices based on average yields achieved under the current climate and those that could be experienced under a range of RCPs. Landowner responses to changing climate

and socio-economic conditions are parameterised using estimates from biophysical models described elsewhere in this paper, commodity prices estimated from CliMAT-DGE, and farm budgeting models described in Daigneault et al.(2014).